Is Breakdown Of Fatty Acid Peroxides Involved In The Induction Of Apolipoprotein A1?

2013

Rajat Gupta
University of Central Florida

IS BREAKDOWN OF FATTY ACID PEROXIDES INVOLVED IN THE INDUCTION OF APOLIPOPROTEIN A1?

by

RAJAT GUPTA
Bachelor of Technology, Thapar University, India, 2010

A thesis submitted in partial fulfillment of the requirements
for the degree of Masters in Science in Biotechnology
in the College of Medicine, Burnett School of Biomedical Sciences,
at the University of Central Florida
Orlando, Florida

Summer Term
2013

Major Professor: Sampath Parthasarathy

ABSTRACT

Over the past few years the number of deaths caused due to cardiovascular diseases has been increasing and is of major concern. In the United States, 75% of cardiovascular-related deaths have been attributed to atherosclerosis. Western diets containing large quantities of peroxidized lipids are considered atherogenic. Heated oil in the form of fried food brings high levels of peroxidized fat and its decomposition products in the diet. Peroxidized lipids are known to increase the susceptibility of serum lipoproteins to undergo oxidation, thereby contributing to the progression of atherosclerosis. The intestinal cells are responsible for the absorption of dietary fatty acid peroxides (FAOOH) which has been reported to enhance anti-atherosclerotic effects by inducing apolipoprotein A1 (apoA1) gene and protein levels. Therefore, there is a void in the knowledge of when to expect “harmful” or “beneficial” effects of dietary lipid peroxides. The formation of toxic products like aldehydes from the decomposition of FAOOH is well documented. On the other hand, carboxylic acids particularly azelaic acid, formed as an end product of FAOOH decomposition has been reported to have anti-atherosclerotic effects. Hence, we hypothesize that intestinal cells may decompose FAOOH to aldehydes, which might get converted to carboxylic acids that can be transported across the intestine. Linoleic acid is the most abundant polyunsaturated fatty acid (PUFA) present in the diet. So, we will use peroxidized linoleic acid (13-HPODE) and incubate with intestine derived cells or Caco-2 cells as an *in-vitro* model for determining its decomposition to aldehydes and carboxylic acids. We propose that the decomposition products of FAOOH in the presence of intestinal cells might be

responsible for causing an increase in apoA1 levels, which might suggest that lipid peroxidation derived products might actually be beneficial for reducing the progression of atherosclerosis as compared to the absorption of intact FAOOH.

ACKNOWLEDGMENTS

First and foremost I would like to express my deep gratitude to my project investigator, mentor and committee chair Dr. Sampath Parthasarathy for giving me an opportunity to work in his laboratory. His vision has given me the chance to work on a novel project. His moral support, trust and invaluable ideas have immensely helped me throughout the project term. I would also like to acknowledge the support and time of my thesis committee members Dr. Shadab Siddiqi and Dr. Mollie Jewett.

A very special thanks to all my lab members: Dr. Dmitry Litvinov, Dr. Chandrakala Aluganti Narasimhulu, Dr. Krithika Selvarajan, Dr. Irene Fernandes-Ruiz, Dr. Dong Zhao and Bhaswati Sengupta for discussing various concepts and techniques involved in my project. They have always been very supportive and I thank them for their valuable time, effort and suggestions.

I also wish to thank Dr. Subhrangshu Guhathakurta and other members from Dr. Yoon-Seong Kim's laboratory for their continuous guidance and support.

I would also like to thank my parents and my brother for giving me tremendous moral support and emotional strength to overcome difficult circumstances. They have provided constant encouragement towards achieving my goals and for making me a responsible person in life.

Above all, I wish to thank god almighty for making this possible and for giving me enough physical and mental strength to achieve my dream.

TABLE OF CONTENTS

LIST OF FIGURES

LIST OF TABLES

CHAPTER-1: INTRODUCTION

1.1 Cardiovascular diseases- statistical update

Over several decades, there has been an increasing concern to control the number of deaths caused due to heart diseases. The center for disease control and prevention (CDC) has reported that about 600,000 people die of heart diseases every year, and is the leading cause of death for both men and women. The most common one is coronary heart disease (CHD), which is responsible for killing more than 385,000 people annually (Minino, Murphy *et al.* 2011). 75% of all cardiovascular related deaths in the US is caused due to atherosclerosis (Lewis 2009). The figures below have been taken from the American Heart Association (AHA) journal depicting the number of deaths due to heart diseases.

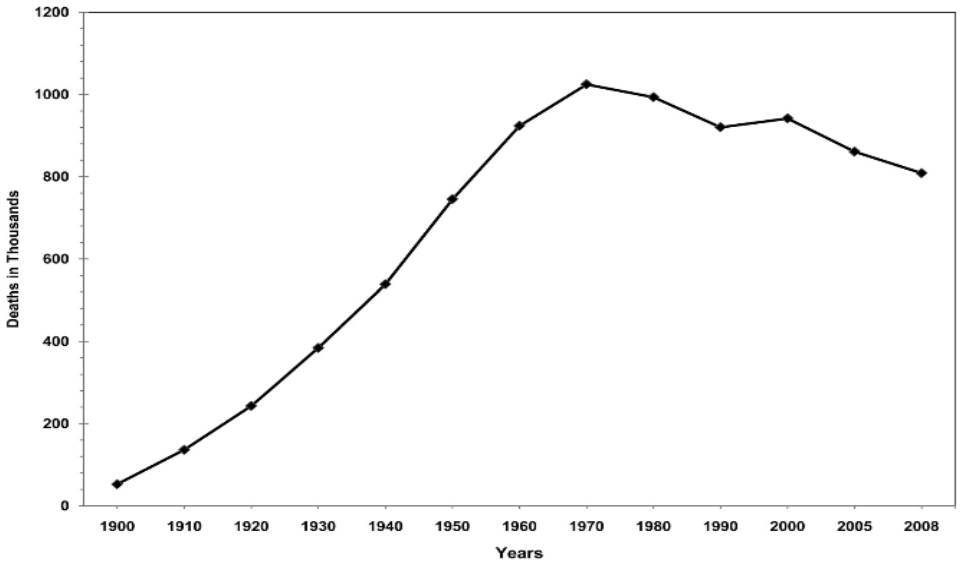

Figure 1-1: Number of deaths caused by cardiovascular diseases from 1900 to 2008.

Although there is a decline in the number of deaths after 1970 till 2008, the numbers still remain very high.

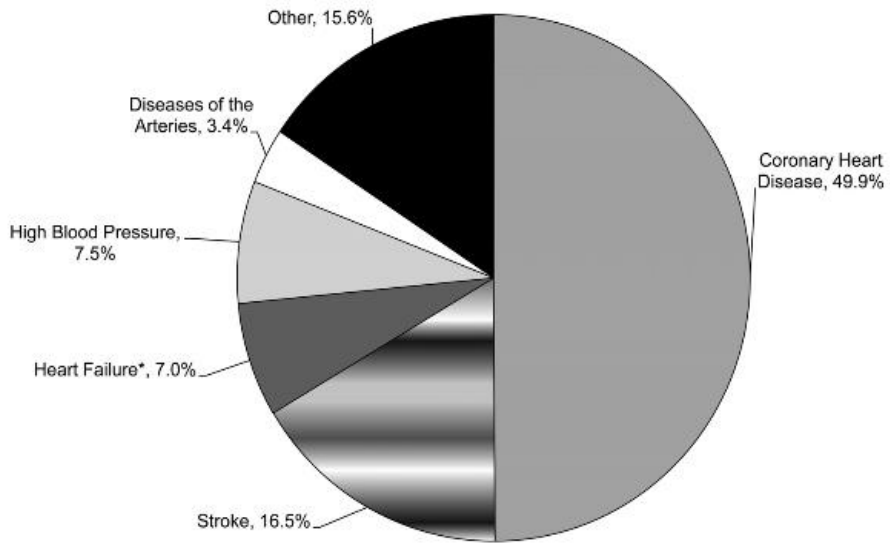

Figure 1-2: Pie chart depicting various causes of cardiovascular related deaths.
Source: National center for health statistics (Roger, Go *et al.* 2012)

1.2 Atherosclerosis

Atherosclerosis is a chronic inflammatory disease caused by the accumulation of cholesterol and its esters in the sub-endothelial macrophages of the artery. It is currently the leading cause of death in the western world societies (Lusis 2000). Several risk factors such as hypercholesterolemia, hyperlipidaemia, hypertension, diabetes mellitus, smoking *etc*. are associated with this disease. Over the past decade, many studies have been carried out to understand the molecular mechanisms in the development of atherosclerotic plaque in genetically modified mouse models. Our laboratory has previously demonstrated that the major cholesterol carrying lipoprotein, low-density lipoprotein (LDL), undergoes oxidative modification which results in the uptake of modified LDL by macrophages leading to foam cell formation (Parthasarathy, Steinberg *et al.* 1992). Atherosclerosis begins during childhood and progresses with

age. The earliest lesions are called ‘fatty streak’ lesions which can be reversible (Massin, Vandoorne *et al.* 2002, Michaelsen, Dyerberg *et al.* 2002). These lesions are a precursor for advanced lesions that can grow sufficiently large enough to occlude the blood flow by formation of thrombus or blood clot resulting in myocardial infraction or heart attack (Lusis 2000).

Inflammation is a major factor in the development of atherosclerosis and inflammatory cells such as monocytes, macrophages and T-lymphocytes play an important role in the process (Ross 1999). Under conditions of oxidative stress/damage to the endothelium, LDL enters into the arterial wall and undergoes oxidative modification. The oxidized LDL (Ox-LDL) can stimulate an inflammatory response by inducing cytokines/chemokines. Adhesion molecules such as intercellular adhesion molecule 1 (ICAM-1) and vascular cell adhesion molecule 1 (VCAM-1) are also induced in the endothelium which can bind to leukocytes and play specific roles in causing rolling, tight adhesion and entry in to the arterial wall in response to chemo-attractant cytokines such as monocyte chemotactic protein 1 (MCP-1). Monocytes enter in to the walls of arteries and differentiate into macrophages. The latter can effectively take up Ox-LDL resulting in the formation of lipid rich foam cells, ultimately giving rise to fatty streak lesions (Lusis 2000, Plutzky 2003, Rader and Daugherty 2008). Vascular smooth muscle cells (VSMC) further migrate towards the intima and begin proliferating, giving out large amounts of collagen resulting in fibrous cap formation under the endothelial cells (figure-1-3). Inflammation is thus enhanced by this process which causes necrotic core formation within the atherosclerotic plaque. VSMC and macrophages are known to

secrete matrix degrading enzymes such as matrix metalloproteinases (MMP) that decrease the stability of plaques making them more prone to rupture. Eventually, plaque rupture leads to the exposure of thrombogenic materials causing thrombus formation, occlusion of blood flow and ultimately resulting in myocardial infraction or stroke.

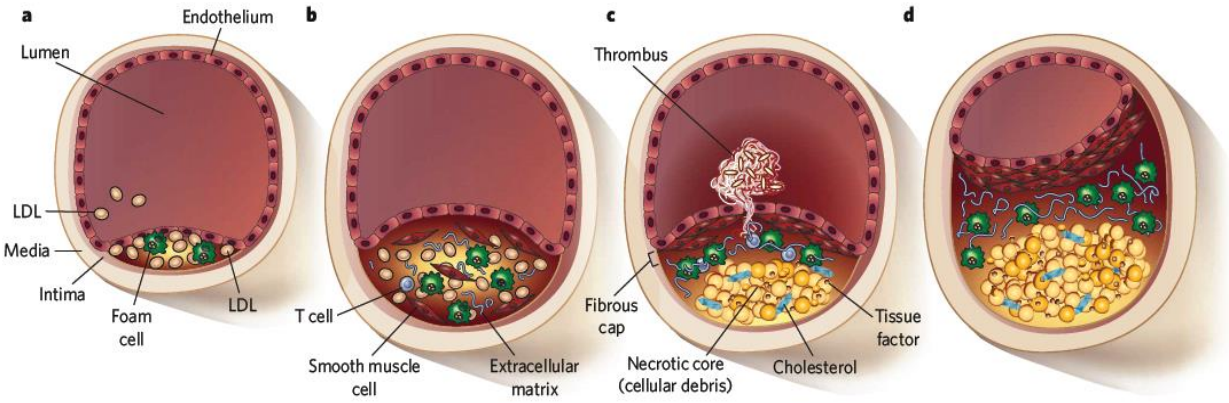

Figure 1-3: Initiation and progression of atherosclerosis.

Early lesions known to develop are called ‘fatty streak’ lesions (a) which can further advance to ‘intermediate’ lesions (b) and then into a lesion vulnerable to rupture (c) and finally leading to occlusion of the arteries (d). (Adapted from Rader *et al.* 2008 (Rader and Daugherty 2008).

1.3 Dietary lipid peroxides and intestinal absorption

Western diets are known to be rich in oxidized fatty acids. Studies have shown that peroxidized lipids enhance atherogenicity of high fat diets (Beltowski, Wojcicka *et al*. 2000). Existing evidences suggest that oxidized lipids present in the diet can contribute to the pool of oxidized lipoproteins that are atherogenic (Steinberg 1997, Staprans, Pan *et al.* 2005). Intestine plays a major role in the absorption of fats present in the diet, by microscopic cell membrane protrusions called microvilli or brush borders. Western diets are rich in polyunsaturated fatty acids (PUFA) that are more susceptible

to undergo oxidation as compared to monounsaturated fatty acids (MUFA). Linoleic acid is the most abundant PUFA present in western diets, which can easily undergo oxidation when subjected to various degrees of processing such as heating, frying and storage of food. This poses a major health risk for individuals. Studies by Staprans *et al.* (1994) have shown that dietary oxidized lipids can be absorbed by the small intestine, transported to the liver *via* chylomicrons, and further get secreted as VLDL, thereby contributing towards the development of atherosclerosis (Staprans, Rapp et al. 1994). Chylomicrons are the lipoproteins that transport ingested fat from the gut to other tissues of the body. Our laboratory has previously demonstarted that intestinal villus cells can take up oxidized fatty acids similar to unoxidized fatty acids and reesterify them by acyltransferases into lipids that constitute the chylomicrons (Penumetcha, Khan *et al.* 2000). Figure-1-4 shows the scheme of events leading to the absorption of triglycerides by the intestine to form chylomicrons (Penumetcha, Khan *et al.* 2000).

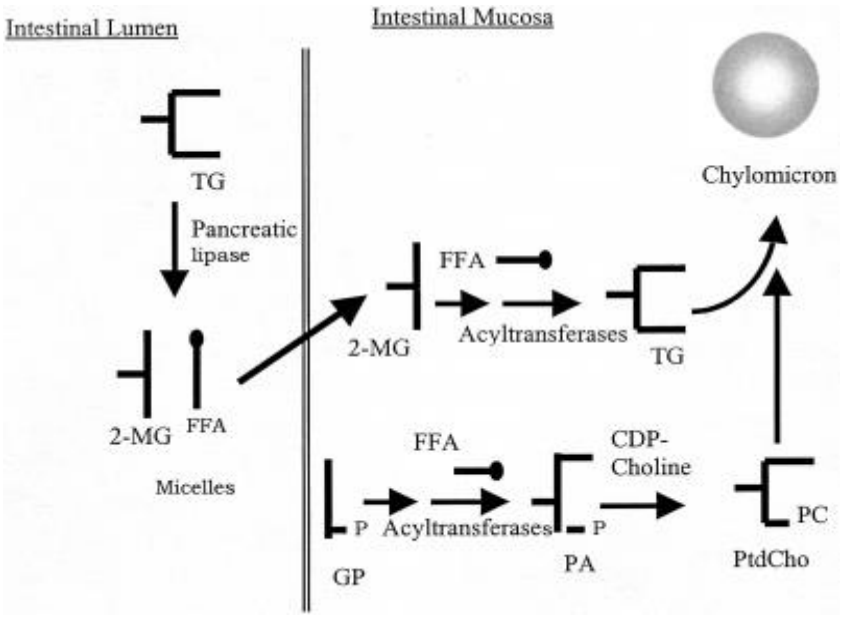

Figure 1-4: Absorption of triglycerides by the intestine.

During the absorption process, triglycerides are acted upon by pancreatic lipase in the presence of bile salts to generate 2-monoacyl glycerol (2-MAG) and free fatty acids. These together with lysophopholipids produced by the action of pancreatic phopholipase on phospholipids present in the diet form mixed micelles favoring efficient absorption into the enterocytes by passive diffusion. Further, acyltransferases reesterify the fatty acids and monoglycerides to generate triglycerides which along with phospholipids constitute a chylomicron. (Adapted from Penumetcha *et al.* 2000 (Penumetcha, Khan *et al.* 2000))

At present, there is a growing need to control the epidemic of obesity and diseases associated with it in the United States and other developed countries. According to the CDC and national health and nutrition examination survey, more than one-third of adults and almost 17% of youth were obese in 2009-10 (Ogden, Carroll *et al.* 2012). Therefore, it is of interest to explore the process of absorption of dietary fat within the enterocytes and its release by the chylomicrons which is well described in a review by Mansbach *et al.* (2010) (Mansbach and Siddiqi 2010).

Upon ingestion of dietary lipids, the fat travels through the esophagus into the stomach where it gets converted into chyme which is further released into the duodenum of the small intestine. Bile acid is then released from the gall bladder that aids in the emulsification of larger fat molecules into smaller droplets that can efficiently be absorbed by the epithelial cells of the gut. The absorption takes place by passive diffusion of the mixed micelles that comprises of lysophosphatidylcholine, cholesterol, free fatty acid (FA), mono-acyl glycerol (MAG) and bile salts. After entering the enterocytes, FA and MAG are transported to the endoplamsic reticulum (ER) with the help of fatty acid binding protein. Within the ER, fatty acid is acylated into its coenzyme A (CoA) derivative that further results in esterification with MAG with the help of an enzyme called monoacylglycerol acyltransferase (MGAT) to form diacylglycerol (DAG). Acetylation of DAG to form triacyl glycerol (TAG) is carried out by an enzyme called acyl-CoA:diacylglycerol acyltransferase (DGAT). Cholesterol also gets esterified to form cholesterol esters (CE) with the help of acyl-CoA cholesterol acyltranferase (ACAT). Further, TAG and CE along with phophatidylcholine get packaged into chylomicrons, and are released to the basolateral membrane for exocytosis into the lamina propria. Finally, they travel into the mesenteric lymph and are released into the circulatory system at the thoracic duct. In the blood stream, chylomicrons acquire two new peripheral apoproteins called apoprotein C (apoC) and apoprotein E (apoE) which are required to bind to the surface of the cell (adipocytes or hepatocytes) for the delivery of triglycerides. Adipocytes express lipoprotein lipase that bind to apoC and cleave triglycerides present in the chylomicrons to FA and MAG which are taken up by the cell.

When the level of triglycerides fall below 20%, apoC gets removed resulting in the formation of chylomicron remnant. These are recognized for uptake by the chylomicron remnant receptor present in the hepatocytes. Fatty acids taken up by the liver are then incorporated into the newly formed very low density lipoprotein (VLDL) and released in circulation.

1.4 Intestinal cells or Caco-2 cells

Caco-2 cells are intestine derived cells obtained from human colon adenocarcinoma that are used as a model system for human intestinal barrier and to study lipid peroxide metabolism. Enterocytes are the main type of cells that are present in differentiated small intestine (Buhrke, Lengler *et al.* 2011). The differentiation is induced by cell-to-cell contact when cultured for 2-3 weeks post confluence. Upon differentiation, these cells develop certain microscopic cell membrane protrusions called microvilli or brush borders (figure-1-5) that participate in the absorption of food and dietary lipid peroxides. Caco-2 cells that are cultured for 14 to 21 days gradually develop brush borders and are hence considered fully differentiated. Whereas, cells cultured for only 4 days or until they become confluent are considered as poorly differentiated cells as they lack brush borders. These are proliferating colon cancer cells that are highly tumorigenic (Buhrke, Lengler *et al.* 2011). The presence or absence of the microvilli is often associated with the increase or decrease in the intestinal alkaline phosphatase (IAP) activity respectively that acts as a marker for differentiation. High expression and activity of IAP is reported in the duodenum (Calhau, Hipolito-Reis *et al.*

1999). Caco-2 cells often grow as a monolayer of cells with tight junctions that indicate a polarized cell layer (Buhrke, Lengler *et al.* 2011). In the human body, cells present at the villus are constantly renewed after 4-8 days by migration of cells along the crypt-villus axis. Hence there exists a fine balance between the cell proliferation, differentiation and apoptosis (Buhrke, Lengler *et al.* 2011).

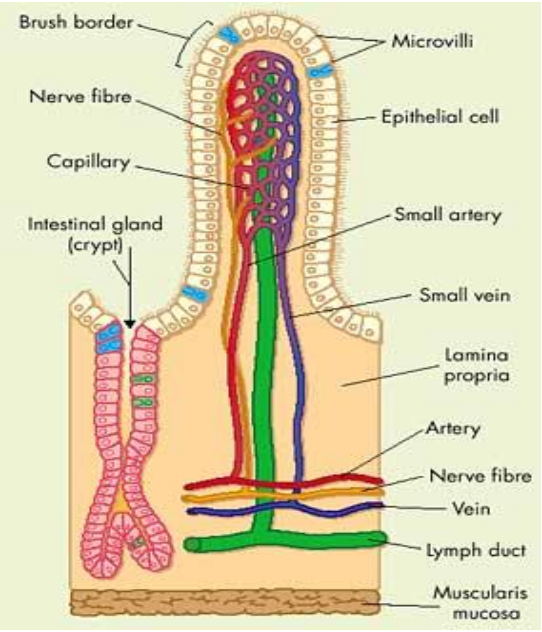

Figure 1-5: Microvillus structure from the cross section of the small intestine.

The outer layer consists of epithelial cells that give rise to brush borders. On the other hand, crypt comprises of proliferating cells present at the base of the villus. Each villus has capillaries into which the nutrients (glucose and amino acids) are absorbed and a lacteal, which absorbs lipids (fats and oils) and drains into the lymph ducts.

Our laboratory has previously shown that cultured cells such as endothelial cells, smooth muscle cells and macrophages take up very little lipid peroxides as compared to unoxidized fatty acids (Auge, Santanam *et al.* 1999). On the other hand, differentiated intestinal cells take up large amounts of oxidized linoleic acid (18:2) which is similar to

unoxidized linoleic acid and oleic acid (Penumetcha, Khan *et al.* 2000). Experiments using radioactive oxidized linoleic acid were done to confirm its uptake by Caco-2 cells is dependent on the presence of brush borders as shown in figure-1-6.

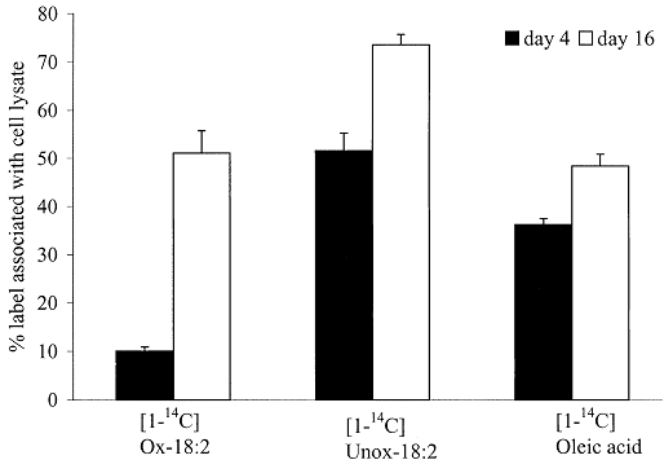

Figure 1-6: Uptake of oxidized and unoxidized fatty acids by Caco-2 cells.

Oxidized linoleic acid ([1-14C]ox-18:2), unoxidized linoleic acid ([1-14C]unox-18:2), and oleic acid ([1-14C]oleic acid 18:1) uptake was measured by 4-day and 16-day old Caco-2 cells upon treatment of 50 nmoles of the three types of fatty acids for 30 minutes. After the incubation, cells were solubilized in deoxycholic acid and an aliquot was taken to determine the radioactivity present in the cell lysate (Adapted from Penumetcha *et al.* 2000 (Penumetcha, Khan *et al.* 2000)).

Linoleic acid present in the diets can form hydroperoxy linoleic acid (13-HPODE: 13-hydroperoxy-9,11-octadecadienoic acid and 9-HPODE: 9-hydroperoxy-10,12-octadecadienoic acid) when oxidized. Previously, our laboratory has demonstrated increased atherosclerosis in oxidized linoleic acid and cholesterol fed LDL-receptor deficient animals (Khan-Merchant, Penumetcha *et al.* 2002).

Recently, studies on understanding lipid peroxidation in association with dietary lipids have gained importance. Our *in-vitro* studies showed that lipid peroxidation leads

to the formation of both aldehydes and their corresponding carboxylic forms (Raghavamenon, Garelnabi *et al.* 2009). Toxic effects of aldehydes like 4-hydroxynonenal (4-HNE) and malondialdehyde (MDA) have been well documented (Devasagayam, Boloor *et al.* 2003). Aldehydes are known to be pro-atherogenic and may induce proliferation of cells at lower concentrations (Aizenshtadt, Burova *et al.* 2011). There is evidence to state that aldehydes can cause covalent modification of the ε-amino groups of the lysine residues of low density lipoprotein (LDL) generating its oxidized form (Haberland, Olch *et al.* 1984, Jurgens, Lang *et al.* 1986, Raghavamenon, Garelnabi *et al.* 2009). On the other hand, some aldehydes like oxo-nonanoic acid (ONA) can get oxidized to dicarboxylic acids like azelaic acid (AZA) that has been shown to inhibit atherosclerosis (Litvinov, Selvarajan *et al.* 2010).

Decomposition of lipid peroxides to aldehydes has been extensively reported, but aldehyde oxidation to carboxylic acids is poorly established. Specifically, aldehyde formation from the ω-end of the fatty acid has gained more attention as compared to the carboxyl end. Our recent studies have shown that 13-HPODE can easily get decomposed to simple aldehydes and carboxylic acids (figure-1-7) when incubated at 37ºC even without cultured cells for up to 72 hours (Raghavamenon, Garelnabi *et al.* 2009).

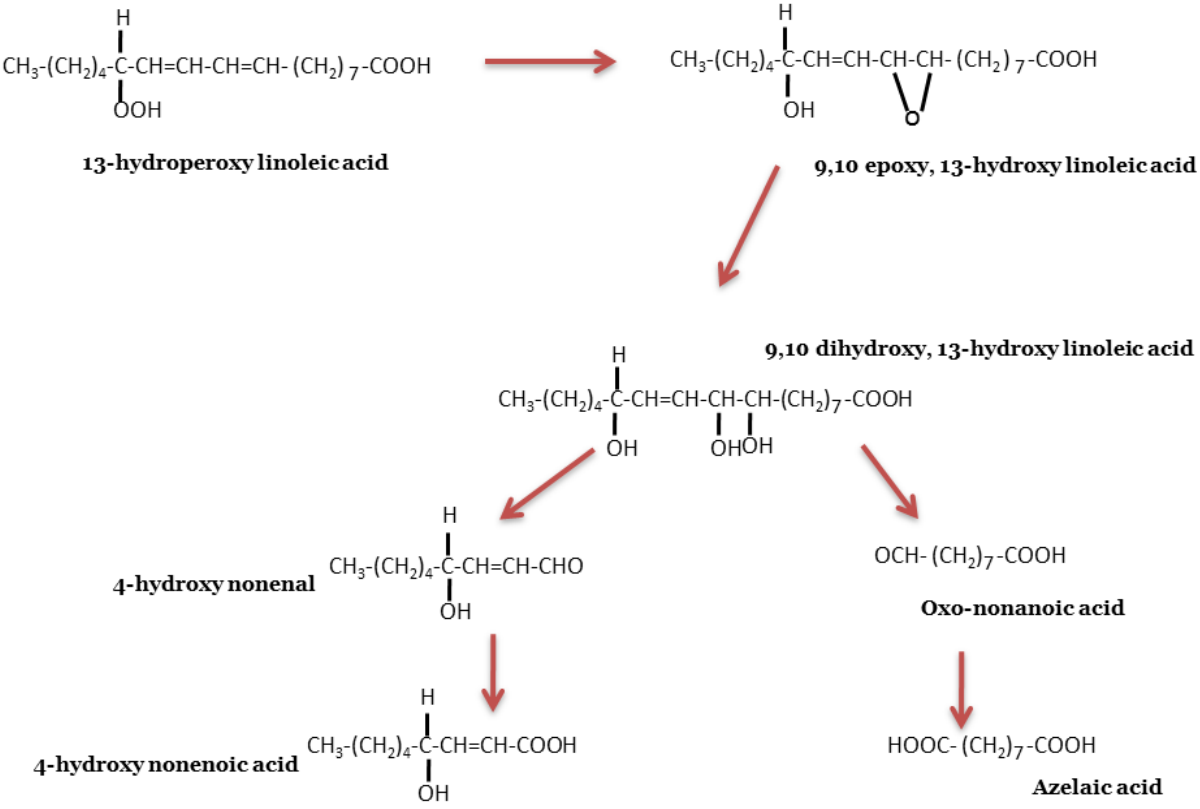

Figure 1-7: Decomposition of 13-HPODE into azelaic acid and 4-hydroxy-nonenoic acid. (Adapted from Raghavamenon *et al.* 2009 (Raghavamenon, Garelnabi *et al.* 2009))

As mentioned earlier, lipid peroxides can be absorbed by fully differentiated cells, but very poorly absorbed by cells lacking brush borders (Penumetcha, Khan *et al.* 2000). Hence based on this, we hypothesize that since intestinal cells are constantly exposed to free fatty acid peroxides (FFAOOH) of dietary origin, aldehydes and carboxylic acids resulting from its decomposition might undergo a different metabolic fate. In the absence of microvilli, cells may breakdown peroxidized fatty acids to

aldehydes, whereas differentiated intestinal cells containing microvilli might either breakdown 13-HPODE to aldehydes which can be converted to carboxylic acids, or absorb the intact fatty acid peroxides. The products may then be transported across the intestine resulting in the generation of anti-atherogenic players such as apolipoprotein A1 (apoA1) in order to combat the toxic effects of dietary lipid peroxides.

1.5 High density lipoprotein, apolipoprotein A1 and reverse cholesterol transport

High density lipoprotein (HDL), also known as “good cholesterol”, is the major lipoprotein responsible for transporting cholesterol from the body tissues to the liver for excretion in the bile (Barter 2000). The process is known as reverse cholesterol transport and is inversely associated with the risk for development of atherosclerosis. The most predominant HDL protein is apoA1 which plays a major role in reverse cholesterol transport and is principally synthesized in the liver and small intestine. Studies by Rubin *et al.* (1991) have demonstrated that cholesterol-fed transgenic mice engineered to produce high levels of human apoA1 develop less atherosclerotic lesions as compared to the wild type mice (Rubin, Krauss *et al.* 1991).

Reverse cholesterol transport involves metabolic pathways for exporting excess cholesterol from foam cells located in the arterial intima for subsequent removal from the body (Brufau, Groen *et al.* 2011, Bandeali and Farmer 2012). In humans, cholesterol can be returned to the liver for excretion by two pathways. Firstly, HDL-cholesterol (HDL-C) can directly bind to the scavenger receptor B1 (SR-B1) expressed on the surface of hepatocytes for a direct hepatic uptake. Secondly, cholesterol esters

can be transferred to apolipoprotein B (apoB) containing lipoproteins, present in circulation by cholesterol ester transfer protein (CETP), followed by hepatic uptake by the low density lipoprotein-receptor (LDL-R) (Fisher, Feig *et al.* 2012). Standard mouse models of atherosclerosis (LDL $r^{-/-}$, $apoE^{-/-}$) when engineered to produce high levels of HDL particles, have resulted in a decreased content of macrophage derived foam cells (Fisher, Feig *et al.* 2012). Apart from carrying out reverse cholesterol transport, several other functions have been ascribed to HDL including anti-inflammatory activity, modification of coagulation parameters, alteration of platelet function and antioxidant activity (Assmann and Gotto 2004, Florentin, Liberopoulos *et al.* 2008, Navab, Reddy *et al.* 2011, Bandeali and Farmer 2012). The structure of HDL (figure-1-8) consists of a monolayer of phospholipids and free cholesterol along with apolipoproteins that function in recognition of receptors, activation of enzymes and conferring structural stability. ApoA1 also serves as a cofactor for the enzyme lecithin cholesterol acyltransferase (LCAT) which is responsible for generating cholesterol esters within the vasculature (Bandeali and Farmer 2012).

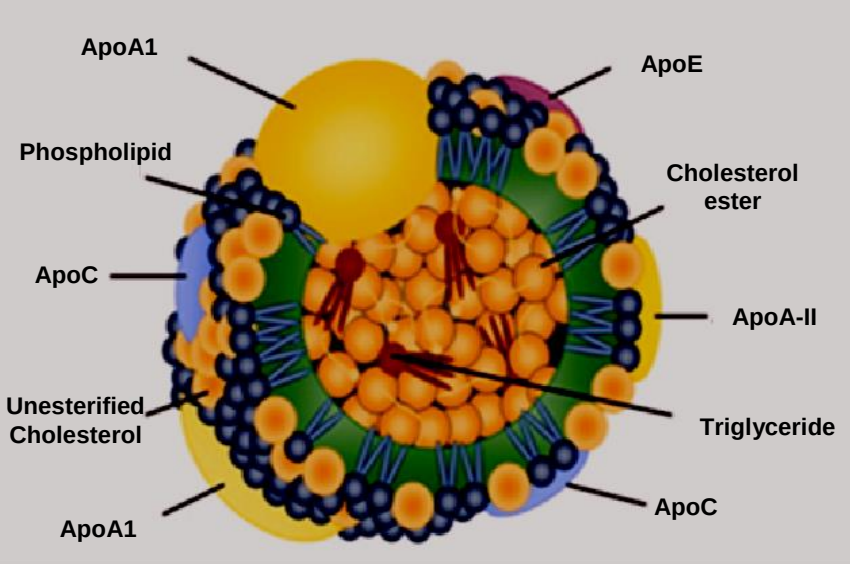

Figure 1-8: Various components present in the mature spherical HDL.

The major apolipoprotein is apoA1 which is present on the surface along with apoC, apoE and apoA-II. Phospholipids and unesterified cholesterol also form a part of the surface. The core mainly consists of triglycerides and cholesterol esters. HDL also contains antioxidant enzymes such as Paraoxonase-1 (PON-1)/Arylesterase-1.

HDL exists in various subforms while present in circulation. Nascent HDL being the precursor, forms a disc like structure and consists of phospholipids and apoA1. These exhibit the capacity to accumulate cholesterol from macrophages by interaction with ATP binding cassette transporters ABCA1 and ABCG1. As the content of cholesterol and phospholipids associated with apoA1 increases, the nascent HDL starts to become more spherical (Navab, Reddy *et al.* 2011). HDL remodeling is also done with the help of phospholipid transfer protein (PLTP) present in the human plasma, that functions to transfer phospholipids from triglyceride rich lipoproteins to HDL (Navab, Reddy *et al.* 2011). In order to be cleared from the plasma, HDL has been known to

acquire apoE which is recognized by the LDL-R (apoB/apoE receptor) present on the hepatocytes for its internalization (Bandeali and Farmer 2012).

Reverse cholesterol transport has been implicated as one of the major pathways to reduce the progression of atherosclerosis by promoting cholesterol efflux. ApoA1 plays a major role in the cholesterol efflux by surface interaction with ABCA1 and ABCG1. It also functions to reduce the oxidative stress in the plasma as shown by overexpression of human apoA1 in apoE knockout mice, which decreased ICAM-1 and VCAM-1 expression, and also decreased the monocyte recruitment into the arterial wall (Theilmeier, De Geest *et al.* 2000, Assmann and Gotto 2004). ApoA1 was also shown to reduce the lipid peroxide levels of phospholipids and cholesterol esters, and also to remove oxidized forms of arachidonic acid and linoleic acid from native LDL, thereby inhibiting the inflammatory response (Navab, Hama *et al.* 2000, Navab, Berliner *et al.* 2001, Assmann and Gotto 2004).

Our laboratory has previously demonstrated that dietary oxidized linoleic acid can induce gene expression and protein levels of plasma apoA1 in intestinal cells in a dose dependent manner (Rong, Ramachandran *et al.* 2002). The induction of apoA1 as measured by ELISA was significantly higher when cells were incubated with oxidized linoleic acid as compared to unoxidized linoleic acid (figure-1-9). This was tested with both poorly differentiated as well as fully differentiated cells of the intestine. The differentiated or 16-day old Caco-2 cells showed a higher dose dependent induction of apoA1 as compared to 4-day old Caco-2 cells. The mechanism of induction of apoA1

might include PPAR-γ with oxidized fatty acid serving as a ligand (Rong, Ramachandran *et al.* 2002).

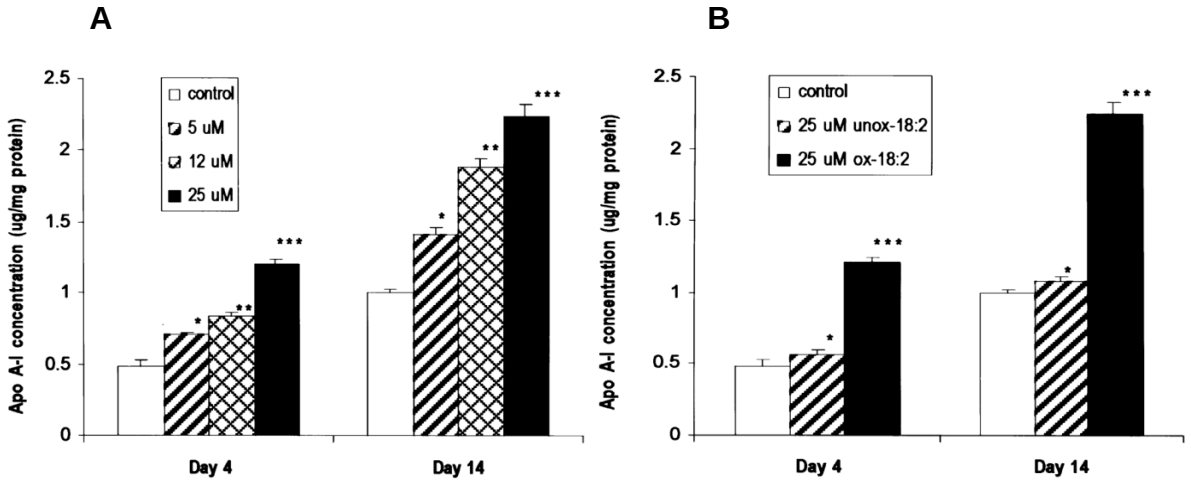

Figure 1-9: Effect of unoxidized and oxidized linoleic acid on the induction of apoA1 protein levels in the cell culture media as measured using ELISA.

Day 4 and day 14 Caco-2 cells were incubated for 20 hours with 25 μM unoxidized linoleic acid (unox-18:2) and 5 μM, 10 μM, and 25 μM oxidized linoleic acid (ox-18:2), with control cells treated with PBS. A: shows the effect of oxidized linoleic acid and B: compares the effect of unox-18:2 with ox-18:2. (Adapted from Rong *et al.* 2002 (Rong, Ramachandran *et al.* 2002)).

1.6 Rationale for the study

Fatty acid peroxides (FAOOH) present in the diets can undergo decomposition to produce aldehydes that can be further oxidized to carboxylic acids (figure-1-10). Oxidation can take place in the presence of free radicals or certain aldehyde oxidizing enzymes such as aldehyde oxidase, aldehyde dehydrogenase and xanthine oxidase.

Figure 1-10: Decomposition of fatty acid peroxides.

The results obtained from our laboratory are summarized as follows:

- Peroxidized free fatty acids can be efficiently taken up by Caco-2 cells and their uptake was dependent on the presence of brush borders (Penumetcha, Khan *et al.* 2000).
- In the presence of peroxidized linoleic acid, differentiated intestinal cells (14-day old) showed increased apoA1 levels as compared to poorly differentiated intestinal cells (4-day old) (Rong, Ramachandran *et al.* 2002).
- Decomposition of peroxidized linoleic acid can generate short chain aldehydes and carboxylic acids (Raghavamenon, Garelnabi *et al.* 2009).

Hence we hypothesize that FAOOH can be either decomposed or transported by intestinal cells and this difference may be determined by the differentiation status of the cells. Poorly differentiated intestinal cells may breakdown FAOOH to aldehydes, whereas differentiated intestinal cells may either breakdown or absorb FAOOH which may in turn induce apoA1, resulting in reduced atherogenesis.

Here we are interested in understanding the decomposition of peroxidized linoleic acid in the presence of Caco-2 cells as well as the effect of its decomposition products on apoA1. We also propose a question whether intact peroxides are absorbed or the aldehydes generated by the decomposition of FAOOH are metabolized by the

intestinal cells that may induce apoA1. Based on evidences, we expect to observe an increase in atherosclerosis, if Caco-2 cells absorb intact 13-HPODE. On the other hand, breakdown of 13-HPODE might be beneficial resulting in increased apoA1 levels.

CHAPTER-2: MATERIALS AND METHODS

2.1 Cell culture and experimental conditions

Caco-2 cells (HTB-37) were purchased from American Type Culture Collection (Rockville, MD). These were cultured in Dulbecco's Modified Eagle Medium (DMEM, Invitrogen #11995-065) supplemented with 15% Fetal Bovine Serum (FBS, Invitrogen #10437-028), 2 mM L-Glutamine (Invitrogen #25030-081), 1% Penicillin-Streptomycin (Invitrogen #15140-122) and 1% Non-Essential Amino Acids (NEAA, Invitrogen #11140-050). After attaining confluence, cells were cultured in the same medium supplemented with 7.5% Fetal Bovine Serum (FBS) while keeping the other constituents same. Confluent cells were trypsinized using 0.25% Trypsin-EDTA solution (Invitrogen #25200-072). Cells were maintained in a 5% CO_2 atmosphere at 37ºC, under sterile conditions.

Caco-2 cells were seeded in 6 well plates and experiments were carried out on days 3-5 and 14-21. In order to ascertain confluence on days 3-5, cells were seeded at a higher density.

2.2 Reagents and antibodies

All routine chemicals were purchased from Sigma (St. Louis, MO). PCR primers and TrizolTM reagent were obtained from Invitrogen (Carlsbad, CA). Human anti-apolipoprotein A1 (Goat) antibody (#600-101-109) was purchased from Rockland Immunochemicals (Gilbertsville, PA). Human anti-β-actin (Mouse) antibody (#A2228-200UL) was obtained from Sigma Aldrich (St. Louis, MO). Horse Radish Peroxidase

(HRP) conjugated rabbit anti-goat antibody (#HAF 017) was purchased from R&D Systems (Minneapolis, MN). HRP conjugated goat anti-mouse antibody (#Sc-2061) was obtained from Santa Cruz Biotechnology (Dallas, TX).

2.3 Preparation of linoleic acid hydroperoxide

Linoleic acid (Sigma #W338001-25G), 200 µM in phosphate-buffered saline (PBS, pH 7.4), was oxidized with the addition of 10 U soybean lipoxygenase (Sigma #L6632-1MU). The oxidation reaction was allowed to complete at room temperature over a period of 1 hour. The formation of conjugated dienes (HPODE) was monitored spectrophotometrically by scanning the absorption between 200 and 300 nm (Uvikon XL, Biotek Instruments, El Cajon, CA), using PBS as the reference. The conversion of linoleic acid into its oxidized form was observed as an increase in the optical density at 234 nm. The freshly prepared 13-HPODE was used immediately in all the experiments.

2.4 Detection of peroxide content using LMB assay

Caco-2 cells were incubated with 25 µM 13-HPODE for 0, 15, 30, 60 and 120 minutes to determine the peroxide uptake by cells. On the day of the experiment, cells were washed and incubated in serum-free medium for 2-3 hours. 13-HPODE was incubated with cells in hanks balanced salt solution (HBSS, Invitrogen #14025-092). After incubation, the medium was harvested and the peroxide levels were determined using leuco-methylene blue (LMB) assay (Auerbach, Kiely *et al.* 1992). Briefly, 200 µL of the LMB reagent was added to 800 µL of the medium and incubated at room temperature for 15-20 minutes. 200 µL sample was aliquoted in triplicates to a 96-well

microtiter plate and absorbance was measured at 660 nm using a microtiter plate reader (Bio-Rad Benchmark Plus). The amount of peroxides were quantitated and plotted on a 2-D bar graph.

2.5 Alkaline phosphatase activity assay

Caco-2 cells cultured in T-75 flasks were harvested gently by adding 1 ml of cold saline and Phenylmethylsulfonyl fluoride (PMSF, Sigma #P-7626) at 40 µg/5 ml and cells were scraped and transferred into a 1.5 ml eppendorf tube. Saline was aspirated after centrifugation of the samples at 700 rpm for 5 minutes at 4°C. The cell pellet was then resuspended in 1 ml of 2 mM Tris (Bio-Rad #161-0716), 50 mM D-Mannitol (Sigma #M9546-250G) containing PMSF at 40 µg/5 ml. Cells were further homogenized using a tissue homogenizer for 15 seconds on ice. The homogenized cell suspension was then centrifuged at 1,000 rpm for 10 minutes at 4°C in order to remove the nuclear membrane. The supernatant was transferred to a 1.5 ml eppendorf tube and protein estimation was carried out using Lowry's assay (Lowry, Rosebrough *et al.* 1951). 100 µg of total cellular protein was incubated with 500 µL of freshly prepared substrate, 7 mM p-nitrophenyl phosphate (Sigma #N3254-5G) in 0.1 M sodium bicarbonate (Fisher Scientific #S233-500), 5 mM magnesium chloride (Sigma #M8266-100G) buffer for 20 minutes at 37°C. The reaction was then quenched by adding 1 ml of 0.1 M solution of sodium hydroxide and read by the UV-spectrophotometer at a wavelength of 410 nm. The absorbance readings obtained were plotted on a 2-D bar graph to compare the

activity of alkaline phosphatase in poorly differentiated and fully differentiated Caco-2 cells.

2.6 Aldehyde dehydrogenase activity assay

Aldehyde dehydrogenase activity assay was performed as described by Guru *et al* (1990) (Guru and Shetty 1990). Growth medium from Caco-2 cells cultured in T-25 flasks at day 4 and day 14 was aspirated and cells were rinsed with 1 ml PBS three times. Cells were then incubated with 1 ml of radio-immunoprecipitation assay (RIPA, Sigma #R0278) buffer at 4°C for 10 minutes for cell lysis to take place. After incubation, cells were scraped off using a cell scraper and the contents were transferred to a 1.5 ml eppendorf tube on ice. The lysate was then centrifuged at 10,000 rpm for 10 minutes at 4°C to pellet the cellular debris and the supernatant was transferred to a new 1.5 ml eppendorf tube on ice. Lowry's assay was then carried out to determine the concentration of proteins in the supernatant. 100 µg of total cellular protein was then added to freshly prepared substrate solution consisting of 0.1 M phosphate buffer at pH 7.2, 10 mM Nonanal (Sigma #76310) and 2 mM β-Nicotinamide adenine dinucleotide hydrate (NAD, Sigma #N1636-100MG). The incubation with the substrate solution was performed for 40 minutes at 30°C. Absorbance was recorded using a microtiter plate reader (Bio-Rad Benchmark Plus) at a wavelength of 340 nm. The absorbance readings obtained were plotted on a 2-D bar graph to compare the activity of aldehyde dehydrogenase enzyme in poorly differentiated and fully differentiated Caco-2 cells.

2.7 RNA isolation

RNA was isolated using TRIzol reagent (Invitrogen #15596018). 1 ml of TRIzol reagent was added to each well of a 6-well plate of Caco-2 cells. Cells were lysed by pipetting the solution up and down several times and the lysate was transferred to a 1.5 ml eppendorf tube. Incubation for 5 minutes at room temperature was performed to ensure complete homogenization and dissociation of the nucleoprotein complex. 200 µL of chloroform was then added to the tubes. The tubes were tightened securely followed by vigorous shaking for 15 seconds. Tubes were allowed to stand for 3 minutes at room temperature followed by centrifugation at 12,000 x g for 15 minutes at 4°C. The aqueous phase was removed carefully and transferred to a new 1.5 ml eppendorf tube, while the lower organic phase was stored at -80°C for isolating proteins. 500 µL of 100% isopropanol was added to the aqueous phase for precipitating RNA. The tubes were incubated at room temperature for 10 minutes. They were then centrifuged at 12,000 x g for 10 minutes at 4°C. The supernatant was aspirated and 1 ml of 75% ethanol was added to the RNA pellet for washing. The sample was vortexed briefly and centrifuged at 7,500 x g for 5 minutes at 4°C. This wash step was carried out three times. RNA was then air dried for 10 minutes and resuspended in 50 µL of RNase free water. RNA concentration was determined using a nanodrop instrument (Thermo Scientific) and was scaled to use exactly 1 µg of RNA for cDNA synthesis.

2.8 cDNA synthesis

cDNA synthesis was carried out using SuperScript III First-Strand Synthesis SuperMix for qRT-PCR kit from Invitrogen (Life Technologies #11752-050). The reagents were thawed and mixed well prior to making the master mix. The following kit components were combined together in a tube on ice:

Table 2-1: cDNA synthesis mix preparation.

Component	**Amount per Reaction**
2X RT Reaction Mix	10 µL
RT Enzyme Mix	2 µL
RNA (1 µg)	x µL
DEPC-treated water	Volume made upto 20 µL
Total Volume	**20 µL**

The RT Enzyme Mix includes SuperScript III RT and RNaseOUT. 2X RT Reaction Mix includes oligo$(dT)_{20}$(2.5 µM), random hexamers (2.5 ng/µL), 10 mM $MgCl_2$, and dNTPs. The contents of the tube were mixed gently and incubated at 25°C for 10 minutes followed by incubation at 50°C for 30 minutes. Further, the reaction was terminated at 85°C for 5 minutes and the tubes were allowed to be chilled on ice. These cycles were carried out in a thermo cycler (VWR). 1 µL (2 U) of *E.coli* RNase H was then added and tubes were further incubated for 20 minutes at 37°C. Finally, samples were stored at -20°C until use.

2.9 Real-Time PCR

For setting up Real-Time PCR, SYBR GreenER qPCR SuperMix for iCycler (Invitrogen #11761-500) was used. The run was carried out on a Bio-Rad iQ5 Multicolor Real-Time PCR Detection System using a 96 well PCR plate (Bio-Rad #2239441). The following components were mixed together to create a master mix for each gene that was analyzed.

Table 2-2: PCR components master mix preparation.

Component	**Amount per reaction tube**
2X SYBR GreenER Supermix	10 µL
Forward Primer, 10 µM	1 µL
Reverse Primer, 10 µM	1 µL
DEPC-treated water	7 µL
Total Volume	**19 µL**

19 µL of master mix was loaded in each well of the PCR plate followed by 1 µL of cDNA. The PCR plate was sealed using a microseal optical adhesive film (Bio-Rad #MSB1001) and centrifuged at 1,200 rpm for 10 minutes at 4°C. The PCR plate was then placed in the iCycler instrument and the PCR was programmed for 1 cycle of 50°C for 2 minutes followed by 1 cycle of 95°C for 8 minutes, 30 seconds. Further, 40 cycles each of 95°C for 15 seconds and 60°C for 1 minute was carried out. Melt curve analysis was performed at 95°C for 1 minute, 55°C for another minute followed by 80 cycles of 55°C ± 0.5°C/cycle for 10 seconds until the temperature reached 95°C. After the run, Ct values and melt curves were analyzed using iQ5 Optical System Software provided by Bio-Rad. The following primers for human targets were used:

Table 2-3: Primer sequences for Real-Time PCR.

Primer	**Sequence (5' to 3')**
ApoA1	Forward: TGGGATCGAGTGAAGGACCT Reverse: CTCCTCCTGCCACTTCTTCTG
Alkaline Phosphatase (ALP)	Forward: CTCACTGAGGCGGTCATGTT Reverse: TAGGCTTTGCTGTCCTGAGC
GAPDH	Forward: AGTCAACGGATTTGGTCGTA Reverse: GGAACATGTAAACCATGTAGTTGAG

The mRNA levels were normalized with respect to corresponding GAPDH gene expression levels.

2.10 Protein precipitation for western blotting

Proteins were precipitated from the phenolic phase of TRIzol harvested cells. DNA precipitation was performed first followed by protein precipitation from the phenol-ethanol supernatant layer. For precipitating DNA, the remaining aqueous phase overlying the interphase was aspirated and 300 µL of absolute ethanol was added. The tubes were capped and mixed several times. The samples were incubated at room temperature for 2-3 minutes. The tubes were then centrifuged at 2,000 x g for 5 minutes at 4°C to pellet the DNA. The phenol-ethanol supernatant was removed and transferred to a new 1.5 ml eppendorf tube. For protein precipitation, 1 ml of isopropanol was added to the phenol-ethanol supernatant and the samples were incubated for 10 minutes at

room temperature. The samples were then centrifuged at 12,000 x g for 10 minutes at 4°C in order to pellet the proteins and the supernatant was discarded. To the protein pellet, 1 ml of wash solution consisting of 0.3 M guanidine hydrochloride (Sigma #50940) in 95% ethanol was added and incubated for 20 minutes at room temperature. The samples were then centrifuged at 7,500 x g for 5 minutes at 4°C and the supernatant was discarded. This wash step was carried out three times. 1 ml of absolute ethanol was then added to the protein pellet and vortexed to dislodge the pellet. The samples were then incubated for 20 minutes at room temperature and centrifuged at 7,500 x g for 5 minutes at 4°C. The supernatant was removed and discarded. The protein pellet was air dried for 5-10 minutes and resuspended in 200 µL of 1% SDS solution. In order to dissolve the pellet completely, samples were incubated overnight at 50°C in a water bath. Next day, the samples were centrifuged at 10,000 x g for 10 minutes at 4°C to sediment any insoluble material. The supernatant containing proteins was transferred to a new 1.5 ml eppendorf tube and protein concentration was determined using Lowry's assay.

Proteins were also isolated using radio-immunoprecipitation assay (RIPA) buffer (Sigma #R0278). This buffer was constituted with protease inhibitor cocktail, PMSF and sodium orthovanadate (Santa Cruz #Sc-24948) by adding 10 µl of each per 1 ml of RIPA on ice immediately prior to use. The growth medium from the cells was gently aspirated and cells were washed twice with 1X PBS to remove minor contaminants. To each well of the 6-well plate, 200 µl of RIPA buffer was added and the plate was incubated on ice for 10 minutes for lysis to take place. The cells were then gently

scraped and the lysate was transferred to a 1.5 ml eppendorf tube on ice. The samples were then centrifuged at 10,000 rpm for 10 minutes at 4°C and the supernatant containing proteins was transferred to a new 1.5 ml eppendorf tube. Protein concentration was determined using Lowry's assay.

2.11 Western blot analysis

Western Blot was carried out for detecting apolipoprotein A1. 12% SDS-polyacrylamide gel was prepared freshly. 15 µg of protein samples were mixed in a 1:1 ratio with Laemmli sample buffer (Biorad #161-0737) constituted with 2-mercaptoethanol (Fisher Scientific #03446-100) and placed in boiling water for 5 minutes. The samples were then allowed to snap cool on ice for 5 minutes, followed by a quick spin down and were loaded along with precision plus protein standard (Bio-Rad #161-0375). Electrophoresis was carried out in 1X running buffer (10X Tris-Glycine-SDS Running Buffer, pH 8.3, 30.2 g Tris base, 144 g Glycine and 10 g SDS for 1 L volume) at 100 V for 2 hours at room temperature. After the run was completed, the proteins were transferred to a PVDF membrane (Bio-Rad #162-0177). Transfer was carried out at 100 V for 2 hours at 4°C in transfer buffer (10X Tris-Glycine-SDS Running Buffer (80 ml), 20% methanol and de-ionized water (720 ml) for a total volume of 1 L). After completion of transfer, membrane was kept for blocking in an orbital shaker at room temperature for 1 hour. 5% non-fat dry milk (Bio-Rad #170-6404) in Tris Buffer Saline-Tween 20 (TBS-T: 12.11 g Tris, 9 g NaCl, 0.1% Tween-20, pH 7.5 for 1 L volume) was used as blocking reagent. After blocking, the membrane was rinsed twice

with TBS-T followed by washing three times for 10 minutes each. The membrane was incubated with apolipoprotein A1 primary antibody (1:4000, vol/vol in blocking reagent) overnight on a shaker at 4°C. Next day, the membrane was washed three times with TBS-T for 10 minutes each and incubated with secondary antibody (anti-goat IgG conjugated to HRP, 1:5000, vol/vol in blocking reagent) for 1 hour on a shaker at room temperature. After 3 washes in TBS-T for 10 minutes each, the signal was detected with a chemiluminescence kit (Bio-Rad Immun-Star Western Kit #170-5070). The membrane was first exposed to this solution, dried and then exposed to an X-ray film (CL-XPosure Film, ThermoScientific #34090). The film was developed using an AFP image film processor and finally the protein bands were identified. The membrane was then stripped in mild stripping buffer (1.5% Glycine, 0.1% SDS, 1% Tween-20, pH 2.2) by washing three times for 10 minutes each on a shaker at room temperature. The membrane was then reprobed with anti-β-actin antibody (1:2000, vol/vol dilution in blocking reagent) for 2 hours shaking at room temperature followed by washing with TBS-T. Secondary antibody was then incubated with the membrane (Goat anti-mouse antibody conjugated to HRP, 1:5000, vol/vol in blocking reagent) for 1 hour on a shaker at room temperature. β-actin was used as a loading control.

2.12 Determination of linoleic acid hydroperoxide breakdown products using thin layer chromatography (TLC)

Linoleic acid hydroperoxide was allowed to decompose in the presence of Caco-2 cells as determined by loss of peroxide content and conjugated dienes measurement. After incubating Caco-2 cells with 13-HPODE for 4 hours, 2 ml of the cell culture

medium was harvested into 13x100 mm glass tubes. The media was acidified with 100 µL of 1N HCl followed by extraction of lipids using 2 ml of diethyl ether (Sigma #296082-1L). The mixture was briefly vortexed and centrifuged at 500 x g for 5 minutes at 4°C. The upper organic phase containing lipids was transferred to a new glass tube and evaporated under nitrogen gas. The resultant residue was dissolved in 15 µL of chloroform twice followed by vigorous vortexing each time, and loaded onto silica G TLC plates (Sigma #Z122777-25EA) using chloroform: methanol (90: 8, vol/vol) as the solvent system. Visualization of the components was carried out with a brief exposure to iodine vapors for unsaturated compounds followed by immersing the chromatogram in bromocresol green reagent (0.2% in ethanol) for detecting organic acids.

Similar experiments were carried out with the radioactive form of linoleic acid (^{14}C-LA, 500 dpm/nmol in ethanol) to determine counts per minute (cpm) in the products formed after incubation with Caco-2 cells. Cells were treated with 50 nmoles of ^{14}C-HPODE per well of a 6 well plate for 4 hours at 37ºC. After incubation, media and cells were harvested separately and lipids were extracted using diethyl ether and chloroform-methanol respectively. Chloroform and methanol were used for extracting cellular lipids according to the method described by Bligh and Dyer (Bligh and Dyer 1959). Briefly, cells were scraped gently in 0.9 ml PBS and homogenized in a dounce homogenizer for 5 minutes. 1 ml of methanol was then added to the homogenate and mixed gently followed by addition of 1 ml of chloroform. This suspension was taken in a glass tube, vortexed and centrifuged at 500 x g for 5 minutes at 4°C. The mixture separates into lower organic phase and upper aqueous phase. The organic phase containing the lipids

was transferred to a new glass tube and evaporated under nitrogen. The resultant residue was dissolved in 15 µL of chloroform twice followed by vigorous vortexing each time, and loaded onto silica G TLC plates. The solvent system used for running TLC was chloroform: methanol: water: acetic acid (65: 25: 3.4: 0.1 vol/vol). Visualization of the components was carried out with brief exposure to iodine vapors for unsaturated compounds, and radioactivity counts were determined by immersing the sections of the TLC plate in scintillation cocktail fluid (Perkin Elmer #6013329) and counts were read overnight in microbeta 2 scintillation counter (Perkin Elmer). Radioactive counts were also determined in the original medium without incubation with cells.

2.13 Saponification of cellular lipids

After incubating ^{14}C-HPODE to Caco-2 cells in a 6-well plate for 4 hours, cellular lipids were extracted and subjected to saponification. The extract was hydrolyzed by adding 0.5 ml of 3 M methanolic potassium hydroxide (KOH) solution and heated at 80°C for 1 hour in a water bath. The solution was then cooled to room temperature and non-saponifiables were extracted with 2 washings of 1 ml diethyl ether. The lower aqueous phase was then acidified using 300 µL of 6 M HCl. Extraction of free fatty acids was carried out with 3 washings of 1 ml diethyl ether. Care must be taken to avoid evaporating the ether phase too extensively in order to prevent loss of fatty acids. These fatty acids were then allowed to run on the TLC plate using chloroform: methanol: acetic acid (90: 10: 1 vol/vol) as the solvent system for separating neutral lipids. Visualization of the components was carried out with brief exposure to iodine

vapors and radioactivity counts were determined by microbeta 2 scintillation counter (Perkin Elmer).

CHAPTER-3: RESULTS

3.1 Alkaline phosphatase activity and gene expression in intestinal cells

Alkaline phosphatase (ALP) is a hydrolase enzyme whose activity and expression is largely associated to the gut, especially to the brush borders of enterocytes. In order to determine whether 14-day old cells are well differentiated as compared to 4-day old cells, ALP activity and gene expression was compared. As shown in figure-3-1, increased ALP enzyme activity and gene expression was observed in 14-day old cells suggesting that these cells were well differentiated (more brush borders) as compared to 4-day old cells.

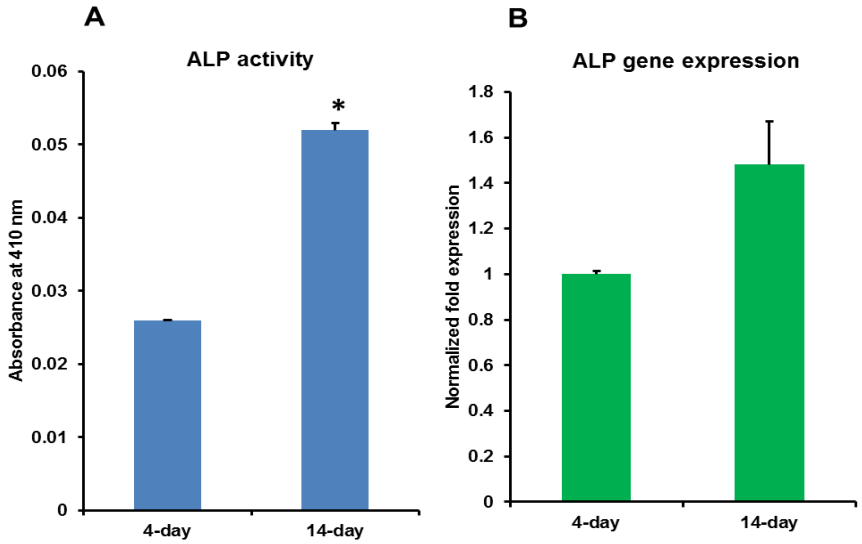

Figure 3-1: Alkaline phosphatase activity and gene expression in Caco-2 cells.

(A) ALP activity in Caco-2 cells. The activity was determined in 100 µg of the total protein lysate from cells by incubating it with the substrate for 10 minutes at 37ºC. The activity in 14-day old cells was significantly higher as compared to 4-day old cells. This experiment was conducted in duplicates with mean ± SE as shown in the figure. **P*<0.01. (B) ALP mRNA levels in Caco-2 cells. RNA was harvested and analyzed. Fold expression was normalized by using glyceraldehyde 3-phosphate dehydrogenase (GAPDH).

3.2 Aldehyde dehydrogenase activity in Caco-2 cells

Aldehyde dehydrogenase is an enzyme that is responsible for oxidizing aldehydes to their corresponding carboxylic forms. The activity of this enzyme was compared in 4-day and 20-day old Caco-2 cells to determine whether aldehydes resulting from lipid peroxide decomposition could be converted in to carboxylic acids. As seen in figure-3-2, fully differentiated cells showed higher enzyme activity as compared to poorly differentiated cells.

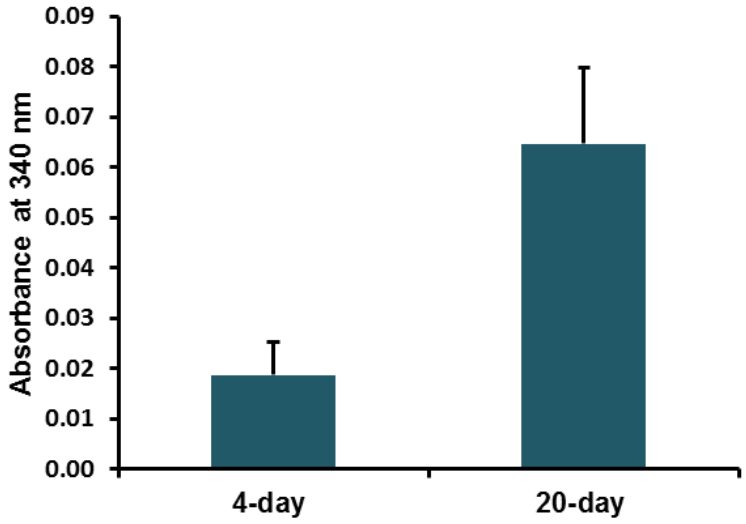

Figure 3-2: Aldehyde dehydrogenase activity in Caco-2 cells.

4-day and 20-day old cells were lysed and 100 µg of total protein lysate was incubated with the substrate at 30ºC for 40 minutes. After incubation, the absorbance was observed at 340 nm to determine enzyme activity.

3.3 Loss of peroxides and conjugated dienes in the presence of intestinal cells

Caco-2 cells were incubated with 50 nmoles of 13-HPODE for various time intervals (0 to 120 minutes) at 37ºC in order to determine the decrease in peroxide content using LMB assay. A 6-well plate without cells (no cells) containing 50 nmoles of

13-HPODE was used to compare the loss of peroxides in the presence of poorly differentiated cells (UND) and fully differentiated cells (DIFF). It was observed that the peroxide content in the cell culture medium gradually decreased with time only in the presence of Caco-2 cells (figure-3-3). This decrease was significant at time points of 30, 60 and 120 minutes.

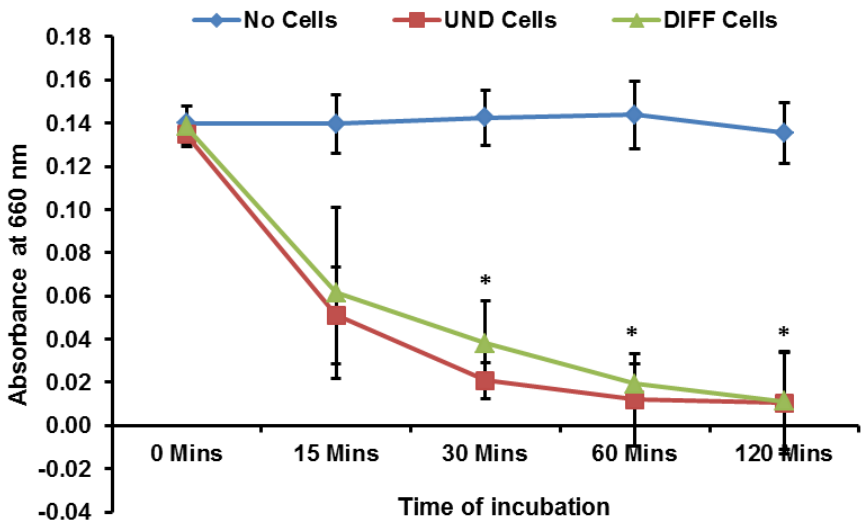

Figure 3-3: Loss of peroxides in the presence of intestinal cells.

The peroxide content in the presence of poorly differentiated (UND) and fully differentiated (DIFF) cells was significantly reduced at 30 minutes, 60 minutes and 120 minutes as compared to no cells. This experiment was conducted in duplicates with mean ± SE as shown in the figure. *P<0.05.

In order to confirm the breakdown of 13-HPODE in the presence of cells, conjugated diene levels were observed at the above mentioned time intervals by performing wavelength scans using a UV spectrophotometer. Immediately after incubation, medium was collected and wavelength spectrums were observed between 200 and 300 nm as shown in figure-3-4. We observed a decrease in conjugated dienes with time only in the presence of cells. Arrows indicate the decrease in absorbance at

234 nm in the presence of cells as compared to no cells. All wavelengths are represented in nm.

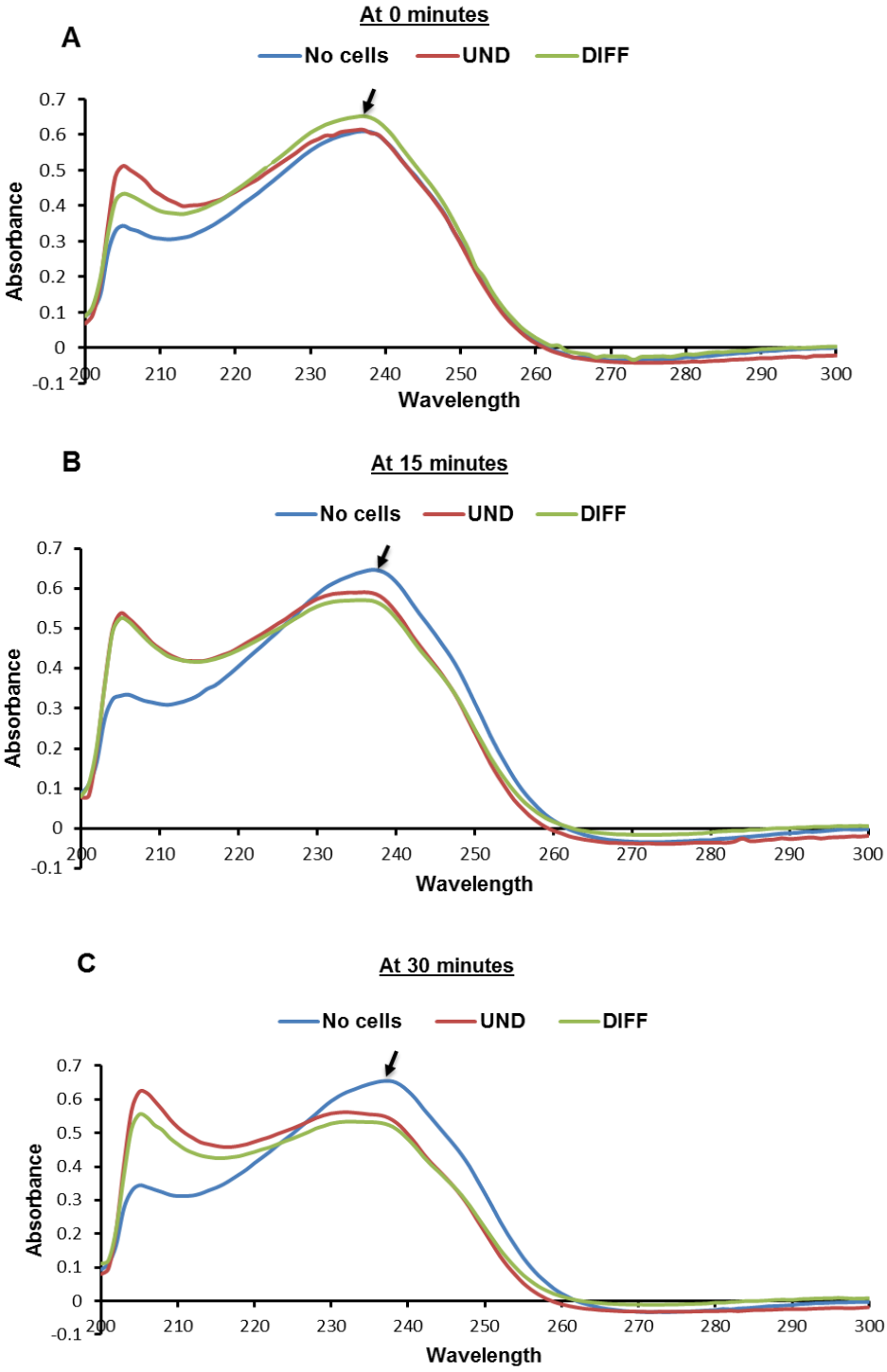

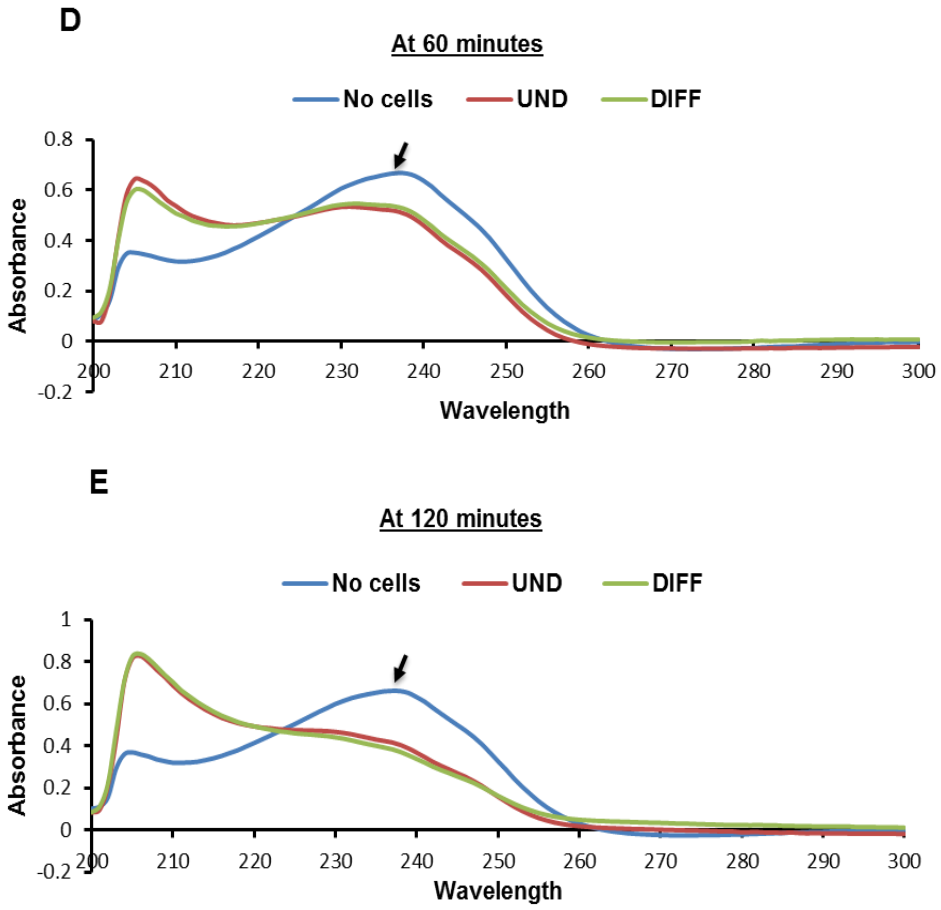

Figure 3-4: Decrease in the levels of conjugated dienes in the presence of intestinal cells.

Figures (A) to (E) represent the conjugated diene levels from 0 to 120 minutes respectively.

Hence, it is clear that 13-HPODE might be either directly absorbed or decomposed in the presence of Caco-2 cells to generate various products. We are particularly interested in the decomposition products generated by Caco-2 cells and whether they would have any impact on apoA1. For this, we used thin layer chromatography (TLC) and radioactive form of 13-HPODE as a means to quantitatively detect the presence of decomposition products in the cells.

3.4 Decomposition products of 13-HPODE in the presence of intestinal cells

Using radioactive counts per minute (cpm) obtained on the TLC plate, the decomposition products of ^{14}C-HPODE were quantified (as percentage cpm) when incubated with Caco-2 cells. In the first experiment, 16-day old cells were incubated with 50 nmoles of ^{14}C-HPODE (in duplicates) for 4 hours followed by lipid extraction from the cell culture medium using diethyl ether. Cellular lipids were extracted as described in methods. As observed in figure-3-5, most of the radioactive counts from cellular sample were obtained at the top most section of the iodine stained TLC plate, indicating the presence of non-polar lipids. We anticipate the presence of triglycerides (TG) that may contain ONA, AZA or 13-HPODE as esterified products (figure-3-5).

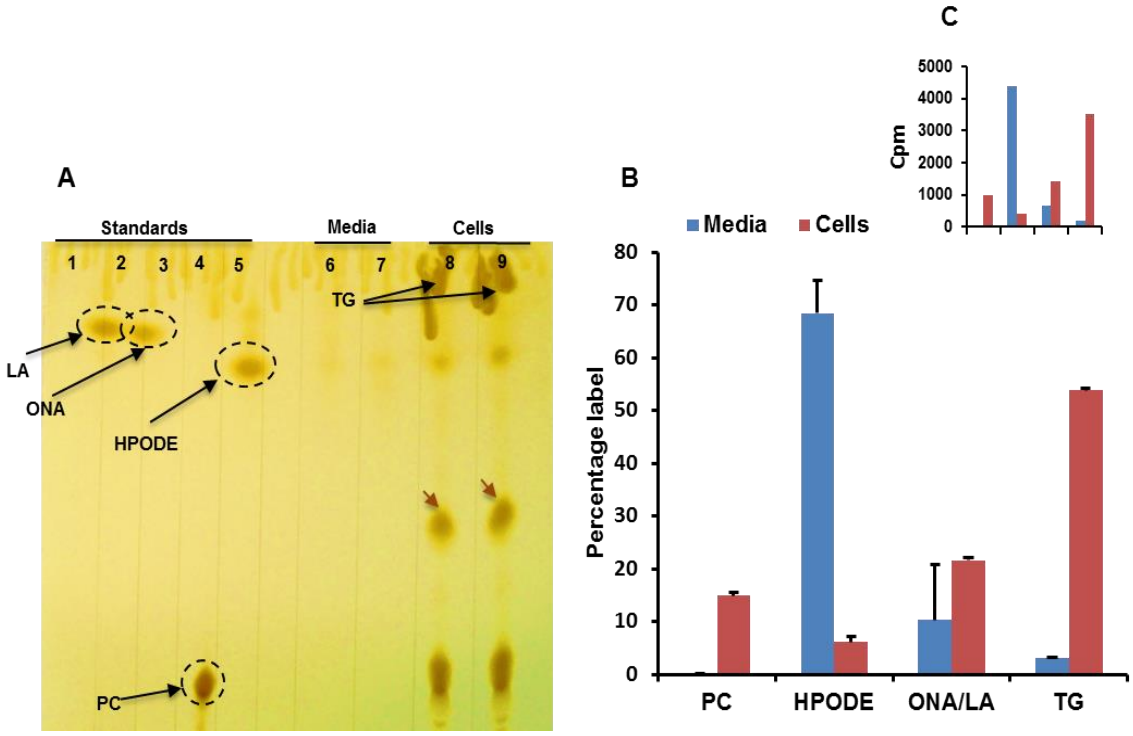

Figure 3-5: Detection of 13-HPODE breakdown products by differentiated Caco-2 cells using thin layer chromatography.

After incubating ^{14}C-HPODE with Caco-2 cells for 4 hours, lipids extracted from the medium and cells (each in duplicates) were loaded on to the TLC plate with following standards: (1) LA- linoleic acid, (2) ONA- oxo-nonanoic acid, (3) AZA- azelaic acid, (4) PC- phosphatidylcholine, and (5) 13-HPODE. (A) Iodine stained section of the TLC plate with appropriate standards and samples. Red arrows indicate phosphatidylethanolamine. (B) Bar diagram showing the percentage radioactive distribution of 13-HPODE breakdown products in the medium (blue bars) and cells (red bars) as determined from the mobility of standards. (C) Cpm values in 13-HPODE breakdown products. The following solvent system was used: chloroform: methanol: water: acetic acid (65: 25: 3.4: 0.1 vol/vol).

In order to determine which free fatty acid is esterified to triglycerides, saponification of cellular lipids was carried out in a separate experiment. Fully differentiated Caco-2 cells cultured in 6-well plate were incubated with 50 nmoles of ^{14}C-HPODE for 4 hours followed by extraction of lipids from the cells and medium (each in

duplicates). Cellular lipids from 2 wells were saponified, and free fatty acids obtained from the hydrolysis of triglycerides and phospholipids were extracted using diethyl ether. Finally, all samples were loaded on the TLC plate and iodine stained spots were identified from the mobility of standards. Cpm values and percentage radioactivity distribution was also quantified (figure-3-6).

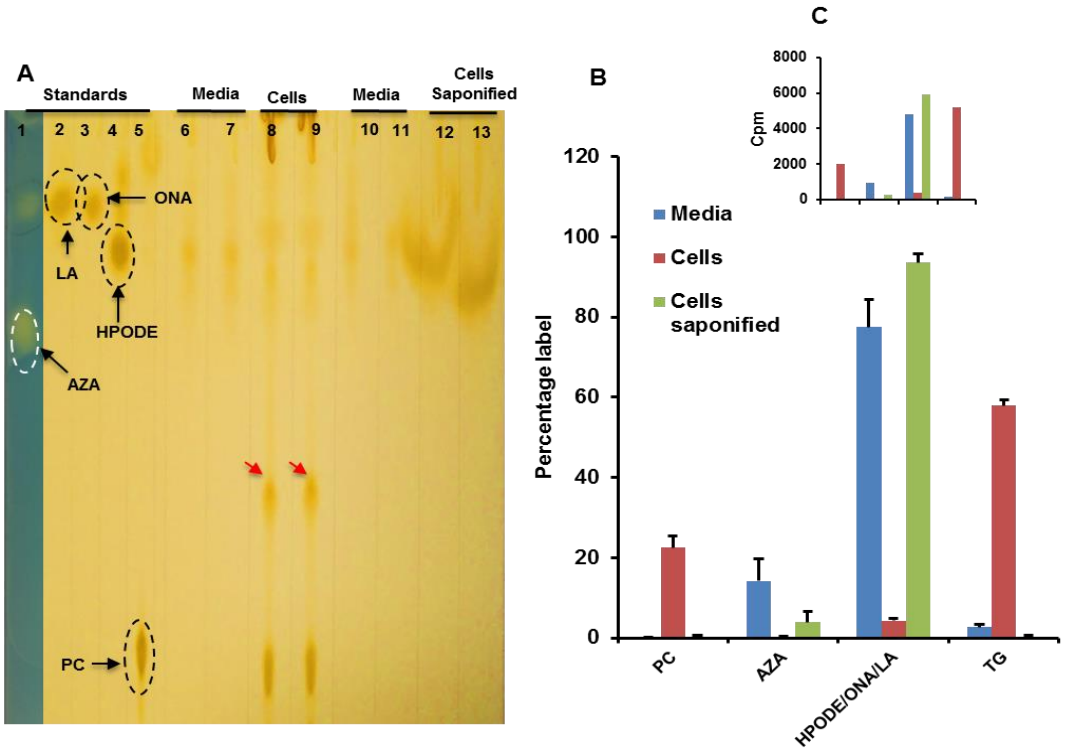

Figure 3-6: Detection of 13-HPODE breakdown products and free fatty acids obtained after saponification of cellular lipids by differentiated Caco-2 cells.

Samples were loaded on the TLC plate after extraction of lipids from cells and media (each in duplicates) along with standards in lanes 1 to 5. (1) Bromocresol green stained section of AZA. (A) Iodine stained TLC plate with appropriate standards and samples. Red arrows indicate phosphatidylethanolamine. (B) Bar diagram showing the percentage radioactivity distribution of 13-HPODE breakdown products in the medium (blue bars), non-saponified cells (red bars) and saponified cells (green bars) as determined from the mobility of standards. (C) Cpm values in 13-HPODE breakdown products. The following solvent system was used: chloroform: methanol: water: acetic acid (65: 25: 3.4: 0.1 vol/vol).

As seen from figure-3-6, the free fatty acid obtained after saponification of cellular lipids was not well characterized due to the appearance of a huge dark spot on the iodine stained TLC plate. Therefore, we chose to use a solvent system that could separate neutral lipids: chloroform: methanol: acetic acid (9: 1: 0.1 vol/vol). Saponified lipids from the cells of the previous batch of fully differentiated Caco-2 cells were again loaded (in duplicates) on the TLC plate along with 13-HPODE and ONA standards (figure-3-7). Iodine stained spots were identified from the mobility of standards, and percentage radioactivity distribution was also quantified as done previously.

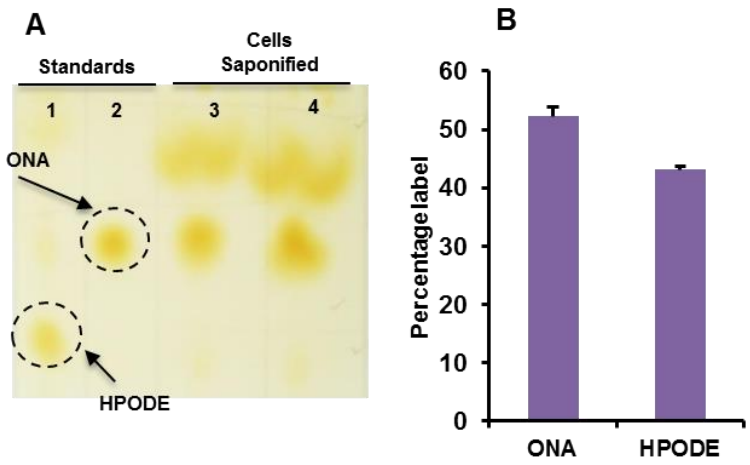

Figure 3-7: Detection of free fatty acids obtained after saponification of cellular lipids by differentiated Caco-2 cells.

(A) Iodine stained TLC plate with appropriate standards and samples. (B) Bar diagram showing the percentage radioactivity distribution of ONA and 13-HPODE in the saponified lipids from the cells as determined from the mobility of standards. The following solvent system was used: chloroform: methanol: acetic acid (9: 1: 0.1 vol/vol).

According to the percentage of radioactive label seen in figure-3-7(B), ONA and 13-HPODE are likely to be esterified to triglycerides when 13-HPODE is incubated with

fully differentiated Caco-2 cells. Since ONA shows higher radioactive counts as compared to 13-HPODE, we anticipate the presence of more ONA molecules getting esterified to triglycerides. In order to determine whether the fate of decomposition products of 13-HPODE by poorly differentiated cells might be any different than that of fully differentiated cells; similar experiment was carried out in the presence of 4-day old Caco-2 cells.

4-day old Caco-2 cells were cultured in a 6-well plate and incubated with 50 nmoles of ^{14}C-HPODE for 4 hours followed by extraction of lipids from the cells and medium (each in duplicates). Cellular lipids from 2 wells were saponified, and free fatty acids were extracted using diethyl ether. Finally, all samples were loaded on the TLC plate and iodine stained spots were identified from the mobility of standards. Cpm values and percentage radioactivity distribution was also quantified (figure-3-8).

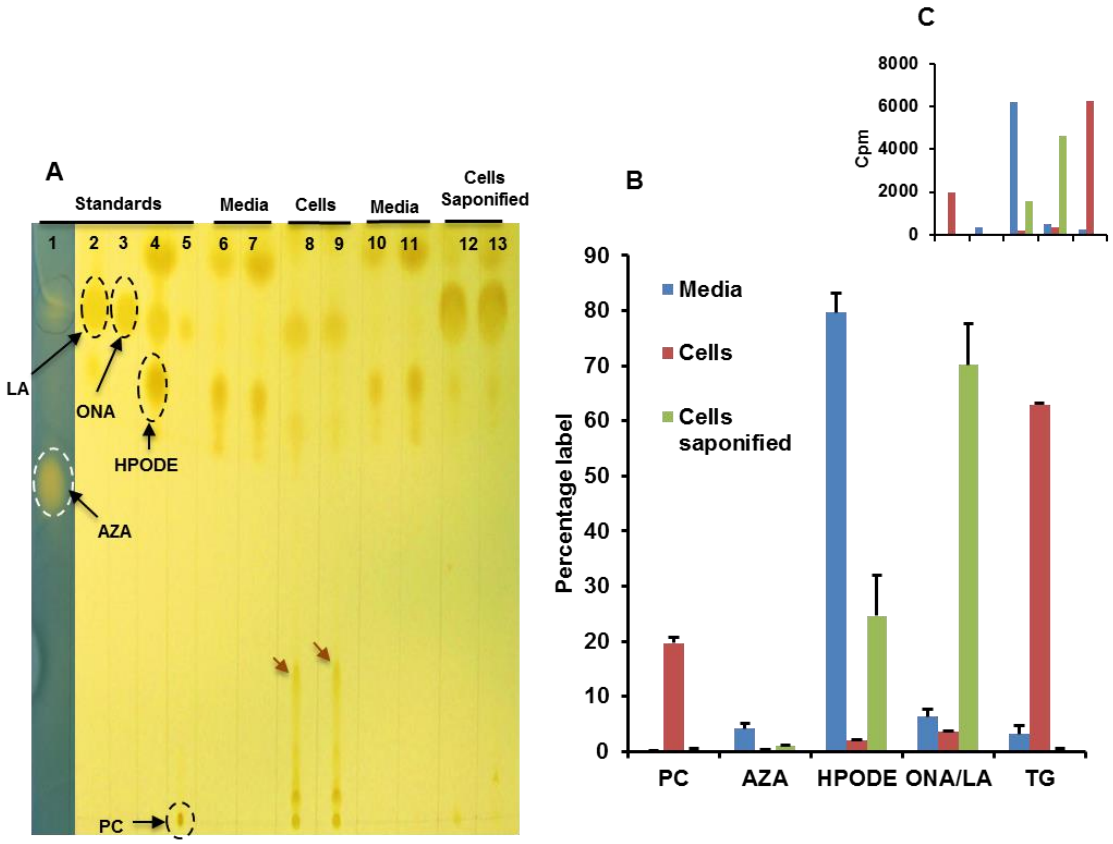

Figure 3-8: Detection of 13-HPODE breakdown products and free fatty acids obtained after saponification of cellular lipids by poorly differentiated Caco-2 cells.

Samples were loaded on the TLC plate after extraction of lipids from cells and media (each in duplicates) along with the previous standards (1 to 5). (1) Bromocresol green stained section of AZA. (A) Iodine stained TLC plate with appropriate standards and samples. Red arrows indicate phosphatidylethanolamine. (B) Bar diagram showing the percentage radioactivity distribution of 13-HPODE breakdown products in the medium (blue bars), non-saponified cells (red bars) and saponified cells (green bars) as determined from the mobility of standards. (C) Cpm values in 13-HPODE breakdown products. The following solvent system was used: chloroform: methanol: acetic acid (9: 1: 0.1 vol/vol).

This shows the existence of ONA as the major esterified product when 13-HPODE is incubated with 4-day old cells (figure-3-8(B)). However, there exists a possibility that linoleic acid (remaining as unoxidized fraction in 13-HPODE preparation) might also be incorporated as esterified lipids in the cells. So in a separate experiment,

^{14}C-HPODE was freshly prepared and was allowed to separate from linoleic acid on the TLC. Further, ^{14}C-HPODE was scraped off from the TLC plate and extracted using chloroform and methanol (9: 1 vol/vol). The isolated ^{14}C-HPODE was assumed to have no traces of linoleic acid. Fully differentiated Caco-2 cells cultured in 6-well plate were incubated with 50 nmoles of purified ^{14}C-HPODE for 1 hour followed by extraction of lipids from the cells and medium (each in duplicates). Cellular lipids from 2 wells were saponified, and free fatty acids obtained from the hydrolysis of triglycerides and phospholipids were extracted using diethyl ether. Finally, all samples were loaded on the TLC plate and iodine stained spots were identified from the mobility of standards. Cpm values and percentage radioactivity distribution was also quantified (figure-3-9).

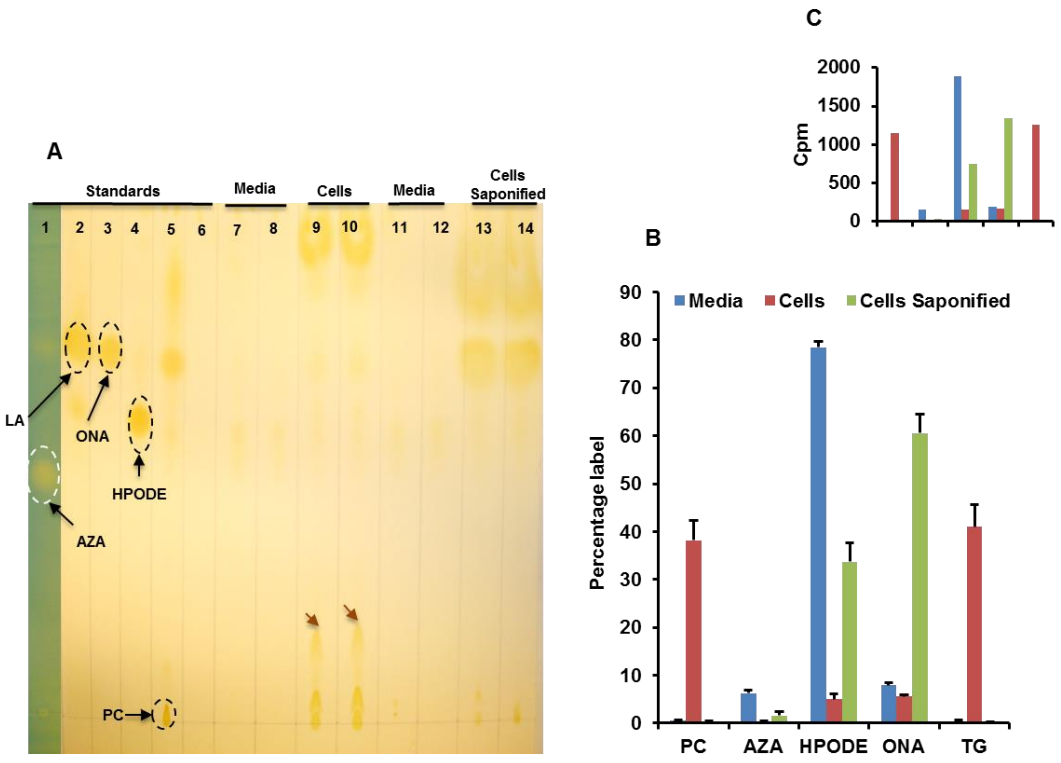

Figure 3-9: Detection of 13-HPODE breakdown products and free fatty acids obtained after saponification of cellular lipids in the presence of pure 13-HPODE by fully differentiated Caco-2 cells.

Samples were loaded on the TLC plate after extraction of lipids from cells and media (each in duplicates) along with the previous standards (1 to 6). (1) Bromocresol green stained section of AZA. (6) Freshly prepared ^{14}C-HPODE. (A) Iodine stained TLC plate with appropriate standards and samples. Red arrows indicate phosphatidylethanolamine. (B) Bar diagram showing the percentage radioactivity distribution of 13-HPODE breakdown products in the medium (blue bars), non-saponified cells (red bars) and saponified cells (green bars) as determined from the mobility of standards. (C) Cpm values in 13-HPODE breakdown products. The following solvent system was used: chloroform: methanol: acetic acid (9: 1: 0.1 vol/vol).

This confirms the presence of ONA as the major esterified product that is formed in the cells when 13-HPODE is incubated in the presence of fully differentiated Caco-2 cells (figure-3-9(B)).

3.5 ApoA1 protein levels in Caco-2 cells following incubation with 13-HPODE decomposition products

In order to determine whether 13-HPODE breakdown products may induce apoA1, Caco-2 cells were incubated with LA, ONA and AZA along with controls: no treatment and 13-HPODE. 100 nmoles of each of these components were used to treat the cells in serum free medium for 24 hours. Protein was isolated from the cells and apoA1 levels were determined by western blotting. Figure-3-10 shows the band intensities of apoA1 with respect to β-actin, which was used as a loading control.

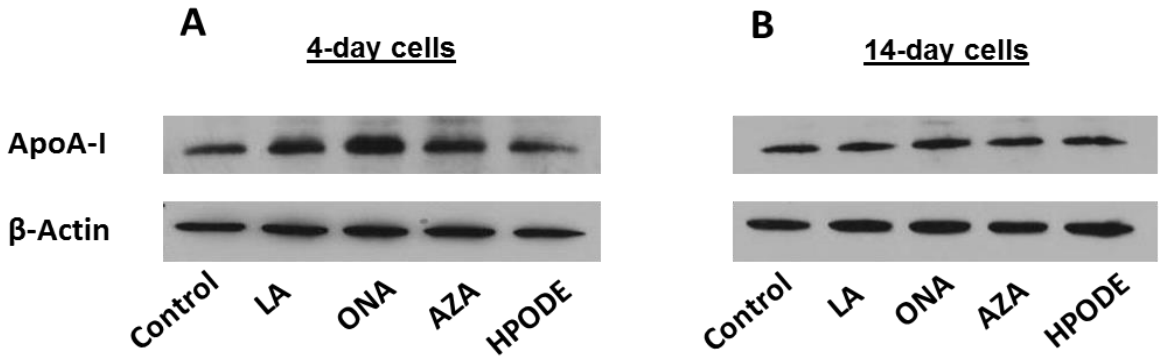

Figure 3-10: Western Blot for apoA1 in Caco-2 cells after incubating with 13-HPODE decomposition products.

Poorly differentiated (UND) and fully differentiated (DIFF) Caco-2 cells were pre-incubated in serum free medium for 2 hours. Cells were then treated with 13-HPODE decomposition products for 24 hours in serum free medium. Western blot analysis was performed with 10 µg of total protein from cell lysates. (A) and (B): Representative polyacrylamide gel of two independent experiments with intensity of bands as seen on the X-ray film after exposure of the PVDF membranes containing proteins to ECL reagents.

Western blot analysis showed that ONA increased apoA1 protein levels in both poorly differentiated and fully differentiated Caco-2 cells.

CHAPTER-4: DISCUSSION

Many studies in the past have suggested that peroxidized lipids present in the diet might be atherogenic (Staprans, Pan *et al.* 1993, Staprans, Rapp *et al.* 1993). Western diets contain large quantities of PUFA that can give rise to peroxidized lipids when subjected to heating at elevated temperatures. This poses a major health risk for individuals who mainly rely on fast food. The small intestine plays a major role in the absorption of dietary lipids and transports them to various tissues in the form of chylomicrons. Evidence from our laboratory suggests that diets containing oxidized linoleic acid can be absorbed by intestinal cells in a similar manner as that of unoxidized linoleic acid (Penumetcha, Khan *et al.* 2000). Since intestinal cells are constantly exposed to dietary ox-FFA, we anticipated whether cells can absorb it directly or break down to generate aldehydes and carboxylic acids.

At present, not much information is available about the fate of peroxidized lipids when exposed to intestinal cells. Some studies suggest that dietary peroxidized lipids can be absorbed by the small intestine, transported to the liver by chylomicrons and further get secreted as VLDL. VLDL is further metabolized to LDL in the plasma and LDL carrying peroxidized lipids could contribute to atherogenesis (Staprans, Rapp *et al.* 1994). On the other hand, studies from our laboratory have shown induction of apoA1 by 4-day and 14-day old Caco-2 cells when incubated with oxidized linoleic acid (13-HPODE) (Rong, Ramachandran *et al.* 2002). These two conflicting evidences might support the fact that if peroxidized linoleic acid is absorbed intact by the intestinal cells, it may be atherogenic. On the other hand, its decomposition to aldehydes and

carboxylic acids in the presence of intestinal cells might actually be beneficial in upregulating apoA1 as a measure to reduce atherosclerotic effects. Thus in the current project, we attempt to determine the decomposition of 13-HPODE in the presence of Caco-2 cells and also pose a question whether its decomposition products may induce apoA1.

In order to study the decomposition of 13-HPODE by intestinal cells, we incubated cells with freshly prepared 13-HPODE and measured the peroxide levels and conjugated dienes at various time intervals. Our preliminary data demonstrated a time-dependent decrease in the peroxide content of 13-HPODE in the cell culture medium when incubated with intestinal cells. We also observed a decrease in the levels of conjugated dienes in the medium with time, indicating that 13-HPODE may either be absorbed by the cells or might undergo breakdown. The possibility of uptake is well established from our current results showing that 14-day old cells are rich in brush borders as compared to 4-day old cells (figure-3-1), and also from previous studies with radioactivity (Penumetcha, Khan *et al.* 2000). The breakdown of 13-HPODE to 4-HNE and ONA (figure-1-7) may be responsible for its loss of conjugated dienes as observed by a decrease in the absorbance at 234 nm (figure-3-4). Since absorption of lipid peroxides takes place through brush borders, we expect that 14-day old cells might readily absorb or breakdown 13-HPODE whereas 4-day old cells may only break it down.

Further, we chose to use radioactive form of 13-HPODE for quantitative measurement of 13-HPODE breakdown products in the presence of cells. 13-HPODE

can be decomposed to generate ONA and 4-HNE which can further get oxidized to AZA and 4-hydroxy nonenoic acid (4-HNA) respectively (Raghavamenon, Garelnabi et al. 2009). Since the carboxylic end of 13-HPODE is radiolabeled, radioactivity in the decomposition products can only suggest the presence of either ONA or AZA. As seen by TLC, cells incubated with ^{14}C-HPODE for 4 hours showed the presence of radioactive products in the lipids extracted from medium as well as cells. After several trials to identify the radioactive products, we found the presence of non-polar triglycerides in the cellular lipids that showed the highest radioactive counts. We also observed high radioactive counts in 13-HPODE spot present in lipids extracted from the medium. Although we have shown that the peroxide content is significantly reduced in the presence of cells (figure-3-3), this might indicate the appearance of conjugated trienes or 13-HODE (13-hydroxyoctadecadienoic acid), a reduced form of 13-HPODE. For the first time we established the existence of esterified products in the cells that are expected to contain free fatty acids generated from 13-HPODE breakdown. This idea was supported by saponifying the cellular lipids in order to identify the free fatty acids formed by hydrolysis of triglycerides and phospholipids. As seen from figures 3-7 and 3-8, high radioactive counts for 13-HPODE and ONA were observed after saponifying the cellular lipids. These products were identified from the mobility of standards under the same solvent system using TLC.

Fully differentiated cells showed almost equal presence of 13-HPODE and ONA as esterified lipids (figure-3-7(B)), whereas poorly differentiated cells showed the presence of more ONA as compared to 13-HPODE (figure-3-8(B)). Thus, the possibility

exists that 14-day old cells may absorb as well as decompose 13-HPODE to ONA which can be further esterified to triglycerides. On the other hand, 4-day old cells may not absorb 13-HPODE as they lack brush borders, but may generate ONA extracellularly that might be incorporated as esterified lipids. It should also be noted that 4-day old cells did not completely lack brush borders and therefore some absorption of intact 13-HPODE was observed.

After determining the presence of decomposition products of 13-HPODE, experiments were conducted to observe their effect on the levels of apoA1. Previous results from our laboratory have shown a dose dependent increase in apoA1 mRNA and protein levels when Caco-2 cells were treated with 13-HPODE. Although fold induction in apoA1 mRNA levels was very less, protein expression was increased as compared to control (Rong, Ramachandran *et al.* 2002). Therefore, we chose to determine apoA1 protein levels by western blotting after treating Caco-2 cells with each of these products.

As seen from figure-3-10, ONA was able to induce apoA1 in both poorly differentiated and fully differentiated cells as compared to control. This suggests that ONA might play a role in reducing atherosclerotic effects by upregulating apoA1 protein levels. Previously, studies from our laboratory have attributed anti-atherosclerotic effects to AZA, suggesting that conversion of lipid peroxidation derived aldehydes to carboxylic acids might be a possible way to prevent oxidative stress (Litvinov, Selvarajan *et al.* 2010). Hence, one may anticipate that ONA might be eventually converted to AZA which may be responsible for anti-atherogenic effects. The oxidation

of aldehydes to carboxylic acid is a common bio-chemical reaction that can occur enzymatically or non-enzymatically. Enzymes such as aldehyde dehydrogenase, aldehyde oxidase, and xanthine oxidase *etc.* can oxidize aldehydes to carboxylic acids. However, in this study there is no evidence to suggest that ONA might be converted to AZA which may further induce apoA1, this is merely an assumption.

The preliminary data obtained in this study needs to be further confirmed by mass spectrometry. This would give a general idea of the products generated by 13-HPODE decomposition in the presence of intestinal cells which may also strongly support our hypothesis. Overall, the results in this study are intriguing and have wide clinical implications for the treatment of patients with advanced atherosclerosis. At this point, it is premature enough to suggest that patients in advanced atherosclerosis stage can be administered short chain carboxylic acids as a means to induce apoA1, which might eventually help in reducing atherosclerosis by promoting reverse cholesterol transport. Further studies are warranted to confirm the current findings.

LIST OF REFERENCES

Aizenshtadt, A. A., E. B. Burova, V. V. Zenin, D. E. Bobkov, I. V. Kropacheva and G. P. Pinaev (2011). "[Effect of formaldehyde in low concentrations on the proliferation and organization of the cytoskeleton of cultured cells]." Tsitologiia **53**(12): 978-985.

Assmann, G. and A. M. Gotto, Jr. (2004). "HDL cholesterol and protective factors in atherosclerosis." Circulation **109**(23 Suppl 1): III8-14.

Auerbach, B. J., J. S. Kiely and J. A. Cornicelli (1992). "A spectrophotometric microtiter-based assay for the detection of hydroperoxy derivatives of linoleic acid." Anal Biochem **201**(2): 375-380.

Auge, N., N. Santanam, N. Mori, C. Keshava and S. Parthasarathy (1999). "Uptake of 13-hydroperoxylinoleic acid by cultured cells." Arterioscler Thromb Vasc Biol **19**(4): 925-931.

Bandeali, S. and J. Farmer (2012). "High-density lipoprotein and atherosclerosis: the role of antioxidant activity." Curr Atheroscler Rep **14**(2): 101-107.

Barter, P. (2000). "CETP and atherosclerosis." Arterioscler Thromb Vasc Biol **20**(9): 2029-2031.

Beltowski, J., G. Wojcicka, D. Gorny and A. Marciniak (2000). "The effect of dietary-induced obesity on lipid peroxidation, antioxidant enzymes and total plasma antioxidant capacity." J Physiol Pharmacol **51**(4 Pt 2): 883-896.

Bligh, E. G. and W. J. Dyer (1959). "A rapid method of total lipid extraction and purification." Can J Biochem Physiol **37**(8): 911-917.

Brufau, G., A. K. Groen and F. Kuipers (2011). "Reverse cholesterol transport revisited: contribution of biliary versus intestinal cholesterol excretion." Arterioscler Thromb Vasc Biol **31**(8): 1726-1733.

Buhrke, T., I. Lengler and A. Lampen (2011). "Analysis of proteomic changes induced upon cellular differentiation of the human intestinal cell line Caco-2." Dev Growth Differ **53**(3): 411-426.

Calhau, C., C. Hipolito-Reis and I. Azevedo (1999). "Alkaline phosphatase and exchange surfaces." Clin Biochem **32**(2): 153-154.

Devasagayam, T. P., K. K. Boloor and T. Ramasarma (2003). "Methods for estimating lipid peroxidation: an analysis of merits and demerits." Indian J Biochem Biophys **40**(5): 300-308.

Fisher, E. A., J. E. Feig, B. Hewing, S. L. Hazen and J. D. Smith (2012). "High-density lipoprotein function, dysfunction, and reverse cholesterol transport." Arterioscler Thromb Vasc Biol **32**(12): 2813-2820.

Florentin, M., E. N. Liberopoulos, A. S. Wierzbicki and D. P. Mikhailidis (2008). "Multiple actions of high-density lipoprotein." Curr Opin Cardiol **23**(4): 370-378.

Guru, S. C. and K. T. Shetty (1990). "Methodological aspects of aldehyde dehydrogenase assay by spectrophotometric technique." Alcohol **7**(5): 397-401.

Haberland, M. E., C. L. Olch and A. M. Folgelman (1984). "Role of lysines in mediating interaction of modified low density lipoproteins with the scavenger receptor of human monocyte macrophages." J Biol Chem **259**(18): 11305-11311.

Jurgens, G., J. Lang and H. Esterbauer (1986). "Modification of human low-density lipoprotein by the lipid peroxidation product 4-hydroxynonenal." Biochim Biophys Acta **875**(1): 103-114.

Khan-Merchant, N., M. Penumetcha, O. Meilhac and S. Parthasarathy (2002). "Oxidized fatty acids promote atherosclerosis only in the presence of dietary cholesterol in low-density lipoprotein receptor knockout mice." J Nutr **132**(11): 3256-3262.

Lewis, S. J. (2009). "Prevention and treatment of atherosclerosis: a practitioner's guide for 2008." Am J Med **122**(1 Suppl): S38-50.

Litvinov, D., K. Selvarajan, M. Garelnabi, L. Brophy and S. Parthasarathy (2010). "Anti-atherosclerotic actions of azelaic acid, an end product of linoleic acid peroxidation, in mice." Atherosclerosis **209**(2): 449-454.

Lowry, O. H., N. J. Rosebrough, A. L. Farr and R. J. Randall (1951). "Protein measurement with the Folin phenol reagent." J Biol Chem **193**(1): 265-275.

Lusis, A. J. (2000). "Atherosclerosis." Nature **407**(6801): 233-241.

Mansbach, C. M. and S. A. Siddiqi (2010). "The biogenesis of chylomicrons." Annu Rev Physiol **72**: 315-333.

Massin, M., C. Vandoorne, C. Coremans, P. Lepage and A. Scheen (2002). "[Preventive cardiology: strategies in children]." Rev Med Liege **57**(4): 207-212.

Michaelsen, K. F., J. Dyerberg, E. Falk, H. S. Hansen, P. Marckmann, O. K. Overvad, L. Schack-Nielsen, F. Skovby and K. E. Sorensen (2002). "[Children, fat and cardiovascular diseases]." Ugeskr Laeger **164**(10): 1334-1338.

Minino, A. M., S. L. Murphy, J. Xu and K. D. Kochanek (2011). "Deaths: final data for 2008." Natl Vital Stat Rep **59**(10): 1-126.

Navab, M., J. A. Berliner, G. Subbanagounder, S. Hama, A. J. Lusis, L. W. Castellani, S. Reddy, D. Shih, W. Shi, A. D. Watson, B. J. Van Lenten, D. Vora and A. M. Fogelman (2001). "HDL and the inflammatory response induced by LDL-derived oxidized phospholipids." Arterioscler Thromb Vasc Biol **21**(4): 481-488.

Navab, M., S. Y. Hama, G. M. Anantharamaiah, K. Hassan, G. P. Hough, A. D. Watson, S. T. Reddy, A. Sevanian, G. C. Fonarow and A. M. Fogelman (2000). "Normal high density lipoprotein inhibits three steps in the formation of mildly oxidized low density lipoprotein: steps 2 and 3." J Lipid Res **41**(9): 1495-1508.

Navab, M., S. T. Reddy, B. J. Van Lenten and A. M. Fogelman (2011). "HDL and cardiovascular disease: atherogenic and atheroprotective mechanisms." Nat Rev Cardiol **8**(4): 222-232.

Ogden, C. L., M. D. Carroll, B. K. Kit and K. M. Flegal (2012). "Prevalence of obesity in the United States, 2009-2010." NCHS Data Brief(82): 1-8.

Parthasarathy, S., D. Steinberg and J. L. Witztum (1992). "The role of oxidized low-density lipoproteins in the pathogenesis of atherosclerosis." Annu Rev Med **43**: 219-225.

Penumetcha, M., N. Khan and S. Parthasarathy (2000). "Dietary oxidized fatty acids: an atherogenic risk?" J Lipid Res **41**(9): 1473-1480.

Plutzky, J. (2003). "The vascular biology of atherosclerosis." Am J Med **115 Suppl 8A**: 55S-61S.

Rader, D. J. and A. Daugherty (2008). "Translating molecular discoveries into new therapies for atherosclerosis." Nature **451**(7181): 904-913.

Raghavamenon, A., M. Garelnabi, S. Babu, A. Aldrich, D. Litvinov and S. Parthasarathy (2009). "Alpha-tocopherol is ineffective in preventing the decomposition of preformed lipid peroxides and may promote the accumulation of toxic aldehydes: a potential explanation for the failure of antioxidants to affect human atherosclerosis." Antioxid Redox Signal **11**(6): 1237-1248.

Roger, V. L., A. S. Go, D. M. Lloyd-Jones, E. J. Benjamin, J. D. Berry, W. B. Borden, D. M. Bravata, S. Dai, E. S. Ford, C. S. Fox, H. J. Fullerton, C. Gillespie, S. M. Hailpern, J. A. Heit, V. J. Howard, B. M. Kissela, S. J. Kittner, D. T. Lackland, J. H. Lichtman, L. D. Lisabeth, D. M. Makuc, G. M. Marcus, A. Marelli, D. B. Matchar, C. S. Moy, D. Mozaffarian, M. E. Mussolino, G. Nichol, N. P. Paynter, E. Z. Soliman, P. D. Sorlie, N. Sotoodehnia, T. N. Turan, S. S. Virani, N. D. Wong, D. Woo, M. B. Turner, C. American Heart Association Statistics and S. Stroke Statistics (2012). "Heart disease and stroke statistics--2012 update: a report from the American Heart Association." Circulation **125**(1): e2-e220.

Rong, R., S. Ramachandran, M. Penumetcha, N. Khan and S. Parthasarathy (2002). "Dietary oxidized fatty acids may enhance intestinal apolipoprotein A-I production." J Lipid Res **43**(4): 557-564.

Ross, R. (1999). "Atherosclerosis--an inflammatory disease." N Engl J Med **340**(2): 115-126.

Rubin, E. M., R. M. Krauss, E. A. Spangler, J. G. Verstuyft and S. M. Clift (1991). "Inhibition of early atherogenesis in transgenic mice by human apolipoprotein AI." Nature **353**(6341): 265-267.

Staprans, I., X. M. Pan, M. Miller and J. H. Rapp (1993). "Effect of dietary lipid peroxides on metabolism of serum chylomicrons in rats." Am J Physiol **264**(3 Pt 1): G561-568.

Staprans, I., X. M. Pan, J. H. Rapp and K. R. Feingold (2005). "The role of dietary oxidized cholesterol and oxidized fatty acids in the development of atherosclerosis." Mol Nutr Food Res **49**(11): 1075-1082.

Staprans, I., J. H. Rapp, X. M. Pan and K. R. Feingold (1993). "The effect of oxidized lipids in the diet on serum lipoprotein peroxides in control and diabetic rats." J Clin Invest **92**(2): 638-643.

Staprans, I., J. H. Rapp, X. M. Pan, K. Y. Kim and K. R. Feingold (1994). "Oxidized lipids in the diet are a source of oxidized lipid in chylomicrons of human serum." Arterioscler Thromb **14**(12): 1900-1905.

Steinberg, D. (1997). "Lewis A. Conner Memorial Lecture. Oxidative modification of LDL and atherogenesis." Circulation **95**(4): 1062-1071.

Theilmeier, G., B. De Geest, P. P. Van Veldhoven, D. Stengel, C. Michiels, M. Lox, M. Landeloos, M. J. Chapman, E. Ninio, D. Collen, B. Himpens and P. Holvoet (2000). "HDL-associated PAF-AH reduces endothelial adhesiveness in apoE-/- mice." FASEB J **14**(13): 2032-2039.